European Union

Ministero dell'Università e Ricerca

University of Cagliari

UNIVERSITY OF CAGLIARI

DEPARTMENT SCIENZE DELLA VITA E DELL'AMBIENTE
MACROSEZIONE DI SCIENZE DEL FARMACO

INNOVATIVE LIPOSOMES FOR OVERCOMING BIOLOGICAL BARRIERS

PhD Program Coordinator:

Prof. Elias Maccioni

Supervisor:

Dr. Maria Manconi

PhD Candidate:

Maura Chessa

PhD Program in:

Tecnologie e legislazione del farmaco e delle molecole bioattive XXV ciclo

S.S.D Chim/09

Acknowledgments

First of all I woukd like to thank my Dr Maria Manconi for the excellent scientific guidance, fruitful discussion, providing me with lab space and equipment. She also gave me the oportunity to partecipate to important conferences. providing me with lab space, equipment and sending me to a number of conferences.

I want to express my sincere gratitude to Prof.ssa Anna Maria Fadda for all the support and guidance throughout all my PhD, and for her enormous generosity.

I would like to express my gratitude to all my collegues of the Department Farmaco Chimico Tecnologico and in particular Prof Chiara Sinico, Francesco, Maria Letizia, Carla, Ines, Checco, Rosa and Francesca for all unconditioned help given during my time in the institute.

Many thanks to Prof. Riccardo Scateni, for helping me in solving computer problems related with my research.

My thanks go to Professor Elias Fattal for giving me the opportunity to spend seven fruitfull month in his laboratory in Paris. In particular I would like to thank all collegues at the University of Paris Sud 11: Hervè Hillaireau, Nicolas Tsapis, Simona Mura, Rym Skanj, Thais Leite Nascimento, Giovanna Giacalone and Chantal Sabbagh for creating an enjoyable and stimulating atmosphere during all of my french research period.

Last but not least, no word can express my sincere gratefulness to my family. Thank you all for your support during the time of this thesis work.

Table of contents

1. General Introduction

Lamellar vesicles are promising drug delivery systems for several pharmaceutical applications and different administration routes. In fact, they offer some advantages over classical dosage forms.

Lamellar vesicles can be divided in two main classes: phospholipids vesicles, called liposomes and introduced by Sir Bangham in 1960 and non-ionic surfactant vesicles, called niosomes as introduced by laboratories l'Oreal in 1970s.

Over the last two decades, the lack of ability of conventional liposomes and niosomes to efficiently deliver drugs through the skin has led to intensive research with the introduction and development of new classes of lipid vesicles.

In the early 1990s, the so called elastic, highly deformable or ultra flexible vesicles were introduced with the aim to improve (trans) dermal drug delivery.

In particular, Transferosomes, introduced by Cevc et al., were the first generation of this new class of lipid vesicles. As with conventional liposomes, they mainly consist of phospholipids but also contain a surfactant (sodium cholate, sodium deoxycholate, different Spans and Tweens, dipotassium glycyrrhinizate) that acts as an “edge activator” capable of destabilizing the lipid bilayer thus increasing its deformability (1).

A second generation of elastic vesicles, mainly consisting of non-ionic surfactants, was introduced in 1999 by van den Bergh (2). Touitou in 2000 developed ethosomes (3), new soft vesicular carriers mainly consisting of phospholipids, water and ethanol in high amount (20-45%). The ethosomes are able to stably encapsulate and protect several drugs and increase their dermal accumulation and transdermal passage (4).

For several years, the group of Technologies for Drug Delivery of the University of Cagliari has been studying delivery of several drugs by liposomes and niosomes. More recently, the group, has introduced the so called Penetration Enhancer-containing Vesicles (PEVs), liposomes containing in their composition a penetration enhancer (PE), as carriers for (trans)dermal delivery of different drugs (5-12). During these years, PEVs have been prepared using various PEs, of different physicochemical properties and mechanism of enhancement, with the aim of finding new stable and efficient vesicular carrier for drug delivery. Moreover, vesicle coating with suitable hydrophilic polymers such as polysaccharide hydrogels, largely studied for their biocompatibility and great versatility in modified drug release, have been studied. In particular, the coating of liposomes with chitosan was found to increase vesicle stability as well as to provide them with mucoadhesive properties (13-15). Thanks to its protective effect, this approach allowed the group to test liposomes for different application such as oral and pulmonary delivery of drugs.

Taking account previous results obtained by my research group, in my thesis research novel vesicular formulations (liposomes and PEVs) are presented for skin delivery of quercetin and phycocyanin, and chitosan coated liposomes (called chitosomes) are proposed for curcumin pulmonary delivery.

Natural antioxidant and anti-inflammatory drugs have received a great deal of attention in recent years for their therapeutic potential for several diseases and low toxicity. The emerging view is that many natural drugs are likely to exert multiple pharmacological effects, in particular the antioxidant and anti-inflammatory properties of these three selected natural drugs have been described by several authors. Unfortunately, the effective efficiency of these naturals is substantially limited by their in vivo low bioavailability. Actually, their gastro-intestinal absorption after oral administration is limited by their low solubility, permeability and/or instability in the gastrointestinal tract (pH, enzymes, presence of other nutrients). As a consequence, their bioavailability at action site is, usually, not enough to exert an effective pharmacological effect, thus, limiting their potential health benefits.

Local administration of these natural drugs into innovative, phospholipids, lamellar vesicles allows circumventing these drawbacks, and would appear to be a promising approach to increase drug bioavailability at action site. In particular, quercetin and phycocyanin can be administrate in the skin to facilitate local drug

delivery to the skin and deeper soft tissues (subcutaneous adipose and skeletal muscle tissue), preventing their systemic side effects.

Topical delivery of drugs has several advantages over other traditional routes of administration, including improved bioavailability for drugs that suffer gastrointestinal environment and/or hepatic first effects. However, the barrier nature of the stratum corneum (SC) represents a significant obstacle for most drugs to be delivered to and through the skin (14). The flattened, anuclear and protein rich corneocytes of the SC are densely packed within the extracellular lipid matrix, which is arranged in bilayers (13). This is often referred to as a 'bricks and mortar' arrangement (15). The corneocytes are held together by corneodesmosomes.

Dermal and transdermal delivery requires efficient penetration of active compounds through the skin barrier by a passive diffusion process. A molecule applied on the skin surface may use two diffusion routes to penetrate: the transappendegeal and the transepidermal routes.

The transappendageal route includes transport via the sweat glands and hairfollicles with their associated sebaceous glands. Although these routes were traditionally considered of minor importance because of their relatively small area, recent research has indicated that the pilosebaceous units may contribute significantly to topical drug delivery by acting as low resistance pathway for ions and large polar molecules which hardly permeate through the stratum corneum.

Moreover, the hair follicles and sebaceous glands are associated with various dermatological disorders such as acne, alopecia, and several skin tumours. Therefore, there is a great interest in the pilosebaceous units as targets for localized drug delivery, as well as shunts for transdermal delivery, even if the specific role of the follicular pathway in dermal drug absorption is difficult to elucidate due to the lack of an adequate animal model to distinguish follicular to non-follicular transport.

Through the epidermis there exist two pathways: the transcellular, across the corneocytes and the lipid matrix, and the intercellular across the lipid domains between the corneocytes.

Structure and barrier function of the skin have been extensively described in the literature and it is generally accepted that the intercellular route provides the principal pathway for the permeation of most drugs.

Molecules are able to move freely within the intercellular spaces and diffusion rates are governed by their physicochemical properties such as molecular weight or volume, solubility and hydrogen bonding ability (17). However, the free movement of macromolecules may be physically restricted within the lipid channels, which have been estimated by van de Merwe et al. to be 19 nm (18) and by Baroli et al. to be 75 nm (19). This suggests that for such materials, the SC could represent an additional barrier that is not present for small molecules.

.

2. Effect of penetration enhancer containing vesicles on the percutaneous delivery of quercetin through new born pig skin.

2.1. Introduction

Quercetin (3,3′,4′,5,7-pentahydroxyflavone, QUE) is a bioflavonoid profuse in nature in plant food sources. It exerts multiple pharmacological effects, including potent anti-oxidant activity in vivo, induction of apoptosis, modulation of cell cycle, anti-mutagenesis, inhibition of angiogenesis, and anti-inflammatory effect. Recently, it has been reported that the topical application of quercetin inhibits oxidative skin damage and the inflammatory processes induced by solar UV radiation (20). Topical use of quercetin is frequently hampered by its low skin permeability and poor solubility in aqueous media, which make the development of pharmaceutical formulations difficult. Different strategies, such as prodrug (21), microemulsion (22), have been used to improve quercetin topical delivery.

In this work, novel quercetin vesicular formulations are presented for skin delivery. Aiming at incorporating quercetin into phospholipid vesicles, four different hydrophilic penetration enhancers (PEs),

essential to improve quercetin solubility in water due to their high solubilizing power, were selected and used to formulate quercetin-loaded Penetration Enhancer containing Vesicles (PEVs). PEV formulations were prepared using 60 mg/ml of a mixture of soy lipids (Phospholipon 50, P50) and one of the selected PEs: Transcutol® P (Trc), propylene glycol (PG), polyethylene glycol 400 (PEG), and Labrasol® (Lab). The use of a mixture of PE/water (40% v/v) as hydrophilic phase, enabled the incorporation of 2 mg/ml of QUE in PEVs without any sign of drug precipitation, during or after fabrication. Previous findings demonstrated that PEVs are powerful enhancers for dermal delivery, due to the synergistic effect of phospholipid vesicles and PE (23, 27). The latter may increase fluidity of the lipid portion of the stratum corneum, facilitating the delivery of the vesicle loaded-drug, and its diffusion through the skin. Given that, quercetin-loaded PEVs were prepared, thoroughly characterized by size, surface charge, loading capacity, morphological and viscoelastic features. Moreover, their penetration capability and distribution through pig skin were assessed by Franz diffusion experiments and confocal microscopy, to give further evidence of the superior performances of PEVs.

2.2. Experimental section

2.2.1. Materials

Soybean lecithin (Phospholipon® 50, P50, with 45% phosphatidylcholine and 10-18% phosphatidylethanolamine) was kindly supplied by AVG (Milan, Italy) and Lipoid GmbH (Ludwigshafen, Germany). 1,2-dioleoyl-sn-glycero-3-phosphoethanolamine-N-(lissamine rhodamine B sulfonyl) ammonium salt (rhodamine-phosphoethanolamine, Rho-PE) was purchased from Lipoid GmbH (Ludwigshafen, Germany). Diethylene glycol monoethyl ether (Transcutol® P, Trc) and caprylocaproyl macrogol 8-glyceride (Labrasol®, Lab) were a gift from Gattefossè (Saint Priest, France). Propylene glycol (PG), polyethylene glycol 400 (PEG), quercetin (QUE) and all the other products were of analytical grade and were purchased from Sigma-Aldrich (Milan, Italy).

2.2.2. Vesicle preparation

QUE (2 mg/ml) was dissolved in a PE/water solution (40% v/v) and added to the flask containing P50 (60 mg/ml). Lipids were left swelling in the solution overnight (28, 29). Sonicated vesicles were prepared by sonicating for 3 minutes (2 seconds on and 2 seconds off) the dispersions with a Soniprep 150 ultrasonic disintegrator (MSE Crowley, UK).

Each vesicle suspension was purified from the non-incorporated drug by exhaustive dialysis against distilled water at 4 °C for 1 hour, using dialysis tubing (Spectra/Por® membranes: 12–14 kDa MW cut-off, 3 nm pore size; Spectrum Laboratories Inc., USA). Incorporation efficiency (E%), expressed as the percentage of the amount of QUE initially used, was determined by high performance liquid chromatography (HPLC) after disruption of vesicles with 0.025% non-ionic Triton X-100. QUE content was quantified at 255 and 367 nm using a chromatograph Alliance 2690 (Waters, Italy). The column was a SunFire C18 (3.5 µm, 4.6x150 mm). The mobile phase was a mixture of acetonitrile, water and acetic acid (94.8:5:0.2, v/v), delivered at a flow rate of 1.0 ml/min.

2.2.3 Vesicle characterization

Vesicles were characterized by Transmission Electron Microscopy (TEM) for vesicle formation and morphology. A drop of the vesicular dispersion was applied to a carbon film-covered copper grid and stained with a 1% phosphotungstic acid. Then, samples were examined with a JEM-1010 (Jeol Europe, France) transmission electron microscope equipped with a digital camera MegaView III and Software "AnalySIS", at an accelerating voltage of 80 kV.

The average diameter and polydispersity index (P.I.) of the samples were determined by Photon Correlation Spectroscopy (PCS) using a

Zetasizer nano-ZS (Malvern Instrument, UK). Samples were backscattered by a helium–neon laser (633 nm) at an angle of 173° and a constant temperature of 25 °C. The P.I. was used as a measure of the width of the size distribution: P.I. less than 0.4 indicates a homogenous and monodisperse population. Zeta potential was estimated using the Zetasizer nano-ZS by means of the M3-PALS (Phase Analysis Light Scattering) technique, which measures the particle electrophoretic mobility in a thermostated cell. All the samples were analysed 24 hours after their preparation.

2.2.4 Rheological studies

Steady shear tests and dynamic oscillatory tests were performed with a controlled strain and stress rheometer (Kinexus pro, Malvern Instruments, UK) equipped with a rSpace data acquisition software. Samples were allowed to rest for at least 300 seconds prior to analyses. Analyses were carried out using a double-gap concentric cylinder DG25 (also called Couette or Coaxial geometry). The test dispersion is maintained in the annulus between the cylinder surfaces. The double-gap configuration is useful for low-viscosity dispersions, as it increases the total area, and therefore the viscous drag, on the rotating inner cylinder, and increases the accuracy of the measurement.

Viscometry experiments were conducted in a shear range of 0.01-10 Pa. Frequency sweep tests were performed from 0.01 to 10 Hz, and at a shear stress of 0.5 Pa. The oscillatory parameters used to compare the viscoelastic properties of the different dispersions were the storage modulus (G'), which represents the elastic part of the response (where energy is stored and used for elastic recoil of the specimen when a stress is removed), the loss modulus (G″), which represents the viscous response (where energy is dissipated and the material flows) (30). All measurements were made in triplicate, at a constant temperature of 25 °C.

2.2.5. Ex vivo skin penetration and permeation studies

Experiments were performed non-occlusively using Franz diffusion vertical cells with an effective diffusion area of 0.785 cm2, and new born pig skin. One-day-old Goland–Pietrain hybrid pigs (~1.2 kg) were provided by a local slaughterhouse. The skin, stored at -80 °C, was pre-equilibrated in physiological solution (0.9% w/v of NaCl) at 25 °C, two hours before the experiments. Skin specimens (n = 6 per formulation) were sandwiched securely between donor and receptor compartments of the Franz cells, with the stratum corneum (SC) side facing the donor compartment. The receptor compartment was filled with 5.5 ml of physiological solution, which was continuously stirred with a small magnetic bar and thermostated at 37±1 °C throughout the

experiments to reach the physiological skin temperature (i.e. 32±1 °C). One hundred microliters of the tested vesicle suspensions, or coarse dispersions of P50, PE and free QUE, were placed onto the skin surface. At regular intervals, up to 8 hours, the receiving solution was withdrawn and replaced with an equivalent volume of pre-thermostated (37°C) physiological fresh solution, to ensure sink conditions. Withdrawn receiving solutions were analyzed by HPLC for drug content.

After 8 hours, the skin surface of specimens was gently washed (3 times) with 1 ml of distilled water, then dried with filter paper. The SC was removed by stripping with adhesive tape Tesa® AG (Hamburg, Germany). Each piece of the adhesive tape was firmly pressed on the skin surface and rapidly pulled off with one fluent stroke. Ten stripping procedures were performed consecutively. Epidermis was separated from dermis with a surgical sterile scalpel. Tape strips, epidermis, and dermis were cut and placed each in a flask with methanol and then sonicated for 4 minutes in an ice bath to extract the drug. The tapes and tissue suspensions were centrifuged for 10 minutes at 10000 rpm, and then the supernatants were filtered and assayed for drug content by HPLC.

2.2.6. Confocal Laser Scanning Microscopy

PEVs were made fluorescent by adding Rhodamine-phosphoethanolamine during the preparation. This labelling allows

visualizing the penetration of the lipid bilayer materials through new born pig skin. (Trans)dermal study was carried out at the same conditions reported in paragraph 2.5. After 8 h of treatment, the skin specimens were washed, the diffusion area punched out, and rapidly frozen at -80 °C. Sections of skin (7 µm thickness) were cut with a cryostat (Leica CM1950, Barcelona, Spain) orthogonally (in the z axis) to the surface, and examined to investigate the fluorescent probe distribution in the different skin strata. Analyses were carried out using a FluoView FV1000 inverted confocal microscope (Olympus, Barcelona, Spain) equipped with a Ultraviolet/Visible light laser. Using a UPlanSApo 20x objective NA 0.75, images with a field size of 1024 × 1024 µm were generated. Rhodamine was excited at 559 nm, and detected at 578 nm. The instrument offers a revolutionary synchronized laser scanning system, called the SIM Scanner: while one laser stimulates, the second laser simultaneously provides high-resolution imaging, which enables the acquisition of images showing the distribution of the marker among skin structures.

2.2.7. Statistical analysis of data

Data analysis was carried out with the software package R, version 2.10.1. Results are expressed as the mean ± standard deviation. Multiple comparisons of means (Tukey test) were used to substantiate statistical differences between groups, while Student’s t-test was

applied for comparison between two samples. Significance was tested at the 0.05 level of probability (p).

2.3. Results and Discussion

In this study, we prepared and characterized phospholipid vesicles containing in the water phase high quantities of different PEs (40%), required to avoid quercetin (2 mg/ml) precipitation. Indeed, we aimed at investigating PEs capability to act as solubilizers for poorly water soluble QUE, and as penetration enhancers for improved (trans)dermal delivery of the drug, synergically with the vesicular carrier system. To this purpose, four different safe, biocompatible, largely used in topical preparations PEs, namely PG, PEG, Lab and Trc were used to formulate as many PEV dispersions, together with P50, a mixture of soy lipids.

2.3.1. Vesicle design and characterization

As mentioned, owing to the extremely poor aqueous solubility of quercetin, a novel delivery approach was designed, that is the preparation of vesicular dispersions. It is noteworthy that it was not possible to obtain conventional phospholipid liposomes (i.e. P50 and QUE in water) with favourable characteristics, due to drug

precipitation. On the contrary, using PE/water blends, novel PEVs were successfully produced.

Vesicle formation in the presence of the PE was confirmed by TEM (Figures 1a-d). PEVs were always multilamellar, showing an irregular and ovoidal shape, except PG-PEVs.

Mean size of PEVs, measured by PCS, was closely related to their composition (Table 1): vesicles containing Trc and PEG were approximately 2.5-3-fold larger than PG- and Lab-PEVs, being around 200 nm the former, and 80 nm the latter. This is clearly in accordance with TEM observation. The difference in size between empty and corresponding QUE-loaded vesicles was related to the composition of the samples: empty and QUE-loaded PEG-PEVs showed the same mean size; loaded PG- and Trc-PEVs were larger than the empty ones; loaded Lab-PEVs were smaller than the corresponding empty vesicles. PEVs were quite homogeneously dispersed and values were always repeatable. Zeta potential values were always highly negative (around −50 mV), indicative of a good storage stability against vesicle aggregation and fusion. Lab-PEVs showed a lower zeta potential (around −30 mV), with and without the drug. QUE incorporation into the vesicles at a percentage ranging from 48 to 75 was achieved by the prepared formulations (E%; Table 1), showing their good loading capacity, which was affected by the used PE. PEG-, PG- and Trc-PEVs showed the lowest E%, as a function of their high hydrophilicity (Pow = 0.000015, 0.12 and 0.7, respectively).

The used PEs are characterized by a relatively high hydrophilicity and show good solvent capability for QUE. However, as a consequence of their molecular structure, the corresponding obtained PEVs exhibited somewhat different features (e.g. size, E%), presumably by virtue of specific interactions with the components of the formulations, related to peculiar properties, such as polarity, partition coefficient, and ability to interpenetrate the lipids.

2.3.2. Rheological behaviour

Macroscopic rheological properties of samples, such as viscosity, elastic or viscous moduli, depend on the strength of particle-particle interactions that occur at supramolecular level, and reflect changes in the microstructure of lamellar vesicles. The vesicle dispersions showed the rheological features normally observed in multilamellar vesicle dispersions. The behaviour of the different PEVs on the shear rate against shear stress was first examined (Figure 2). For all samples, the shear rate increased when the shear stress increased, and shear viscosity (= shear stress/shear rate) was independent of the applied shear stress, like for Newtonian fluids. Indeed, in a Newtonian fluid, the relation between the shear stress and the shear rate is linear, the constant of proportionality being the coefficient of viscosity. The viscosity of PEVs was higher than that of water (1 mPa s): approximately 5, 6, 9 and 40 mPa s for Trc-, PG-, PEG- and Lab-

PEVs, respectively. This increase in viscosity is due to the existence of vesicular lamellar structure occupying a high hydrodynamic volume, especially for Lab-PEVs, that showed a smaller size, lesser number of bilayers, and an increased volume fraction occupied by the vesicles, closely related with the increase of viscosity.

In addition, we performed oscillatory frequency experiments to determine the storage (G') and the loss (G") response of the vesicular dispersions to the applied force. In figure 3 representative mechanical spectra of samples are plotted against frequency, in comparison with water. It was found that Trc-PEVs, as well as PG- and PEG-PEVs, disclosed the same behaviour of water, a purely viscous fluid. For these formulations, elastic modulus increased uniquely due to the inertia effect, while the viscous modulus was a little higher than that of water, as evidenced by the viscometry study. On the contrary, Lab-PEVs showed a higher loss modulus (by about 1 order of magnitude with respect to water) and a storage modulus only slightly higher than that of water, indicating the presence of an elastic component, even if the viscous one predominated.

Further, it was evident that the loss modulus (G") was significantly higher (by about 3 orders of magnitude) than the storage modulus (G') throughout the employed frequency range, confirming the viscous nature of PEVs. The smaller magnitude of the elastic modulus indicates weak particle–particle interactions. Therefore, the samples showed the typical behaviour of diluted spherical multilamellar

vesicle dispersions, where the storage modulus is lower than the loss modulus (G' < G") (31), indicating the viscous nature of the samples. Each sample showed different values of viscosity, storage and loss moduli because the different PEs in the vesicle dispersions caused different degrees of swollen lamellar phase.

These results are consistent with the nature of the tested samples: they are diluted dispersions, which behave as ideal Newtonian fluids that simply flow when subjected to a stress, as they are non-structered systems with weak vesicle interactions. On the other side, the presence of labrasol probably makes the vesicular bilayer more deformable, resulting in an increase of the elastic component.

2.3.3. Ex vivo skin penetration and permeation studies

The skin penetration ability of quercetin loaded in PEVs was probed by ex vivo Franz diffusion studies on new born pig skin. The amount of drug accumulated into stratum corneum, epidermis, and dermis is expressed as the percentage of the drug applied onto the skin. As illustrated in Figure 4a, all PEVs promoted QUE deposition in the three main skin strata, showing the same behaviour in all samples: the lowest drug accumulation in the stratum corneum, the highest in the epidermis, slightly higher in the dermis than in stratum corneum, and significantly lower in receptor fluid than in epidermis. In particular,

PG- and PEG-PEVs allowed the highest drug accumulation into (~ 67%) and through (~ 27%) the skin.

To clarify the role of the studied vesicles in (trans)dermal drug delivery, and in particular to elucidate if they act as carriers or penetration enhancers, coarse dispersions of the same composition used to produce vesicles were tested, too. As can be seen in Figure 4b, when the coarse dispersions were used, the drug accumulated in the skin layers was lower: about 6-fold for PG-, PEG- and Lab-PEVs, 20-fold for Trc-PEVs, than that obtained with the corresponding QUE-loaded vesicular formulations, or even nil in the stratum corneum in the case of PG- and PEG-PEVs treated skin. None of the coarse dispersions with free QUE was found to determine a systemic drug permeation. Results obtained confirm PEVs' capability to behave as true carriers, and not simply as penetration enhancers (24, 25).

2.3.4. Confocal Laser Scanning Microscopy (CLSM)

PEVs were labelled with Rho-PE and applied onto pig skin for 8 hours. The fate of the fluorescent bilayer materials through new born pig skin was visualized using the CLSM technique. Mechanical cross-sections were made othogonally to the skin surface, to obtain a good estimation of distribution pattern of fluorescent phospholipids. These cross-sections provided on a single focal plane a simultaneous visualization of stratum corneum, viable epidermis and dermis. Figure

5 consists of 4 cross-sections (~ 400 µm) of pig skin treated with labelled PEVs containing alternatively PG, PEG, Lab or Trc. Images indicate a high accumulation of Rho-PE in the SC (~ 70 µm in depth), since most of the vesicles penetrate into the stratum corneum and fuse with the intercellular lipids. Indeed, phospholipid vesicles disorder the complex structure of the upper intercellular lipid sheets, but also cause an occlusive effect, which helps hydratation of the keratin layer, resulting in an increased penetration. The free drug could easily penetrate into the viable epidermis, but also drug-loaded intact vesicles are facilitated in their passage through the skin, carrying and delivering the drug to the viable epidermis and dermis. Overall, fluorescence in the 4 skin cross-sections was always higher in SC than in epidermis and dermis; PEG-PEVs treated skin showed a high fluorescence also in epidermis; PG- and Trc-PEVs promoted Rho-PE accumulation in the dermis, whereas Lab-PEVs treated skin specimen showed only a slight fluorescence in the dermis. In the light of these findings, PEVs seem to be able to penetrate intact the skin reaching the lowest SC layers where they form a depot from which the drug can be released (24, 32, 33).

Table 1. Characteristics of empty and QUE-loaded PEVs: mean diameter (MD), polydispersity index (P.I.), zeta potential (ZP) and incorporation efficiency (E%). Each value represents the mean ± S.D., n = 6.

		MD (nm)	P.I.	ZP (mV)	E (%)
P50/PG	Empty	52±10	0.36	-51±7	
	QUE	83±10	0.35	-63±4	57±8
P50/PEG	Empty	193±5	0.30	-51±2	
	QUE	190±4	0.31	-58±2	48±7
P50/Lab	Empty	135±10	0.27	-21±4	
	QUE	86±5	0.29	-32±3	75±9
P50/Trc	Empty	156±6	0.19	-51±6	
	QUE	226±5	0.28	-49±5	59±8

Figure 1. Negative stain electron micrographs of QUE-loaded PEVs prepared with: (a) propylene glycol, (b) PEG400, (c) labrasol, (d) transcutol.

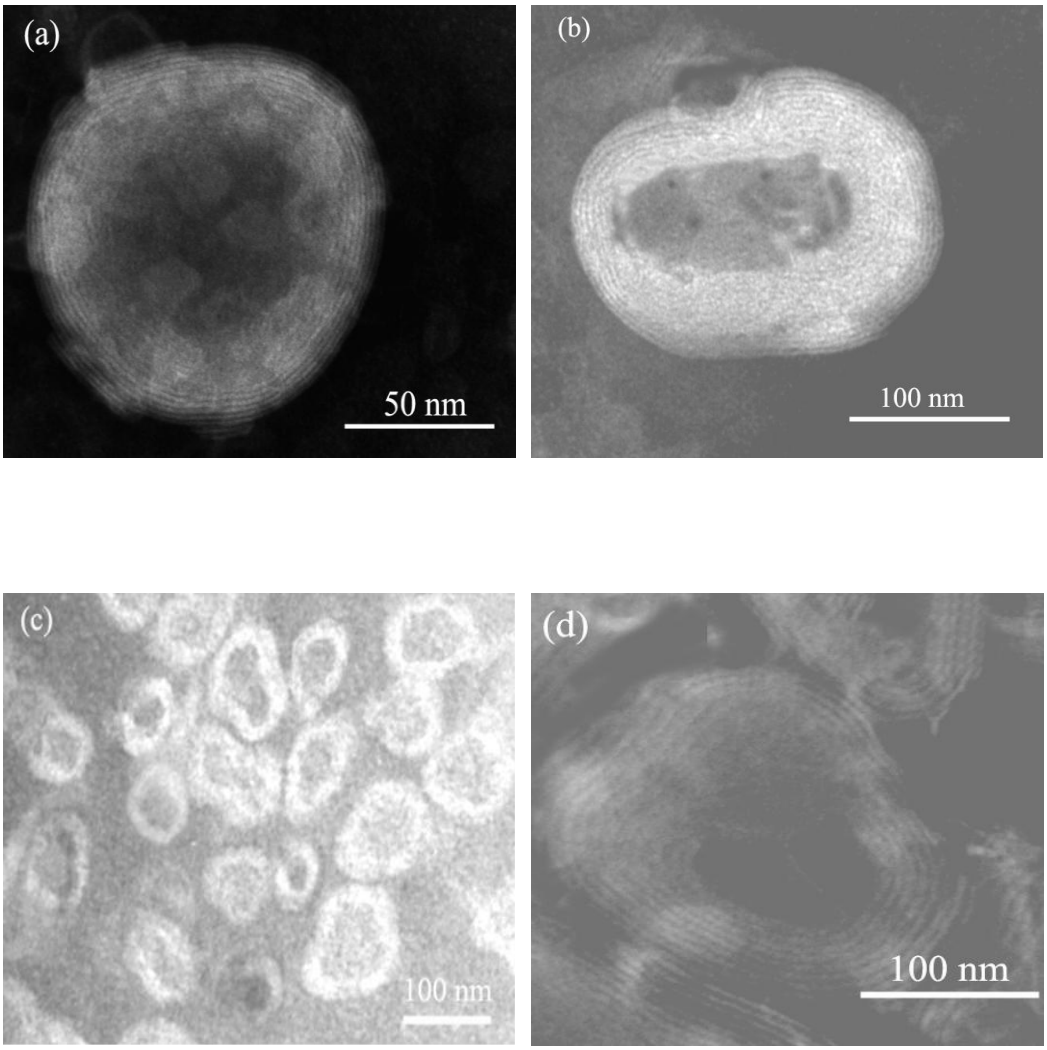

Figure 2. Linear scale plots of shear rate vs shear stress for QUE-loaded PEVs

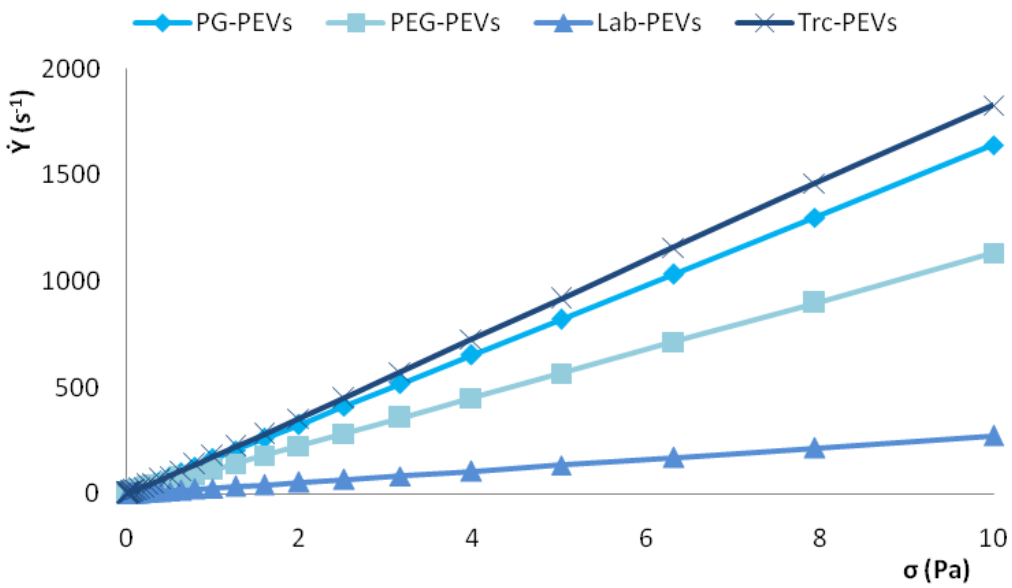

Figure 3. Frequency sweep spectra for PEVs: storage (G') and loss (G") moduli against frequency are shown

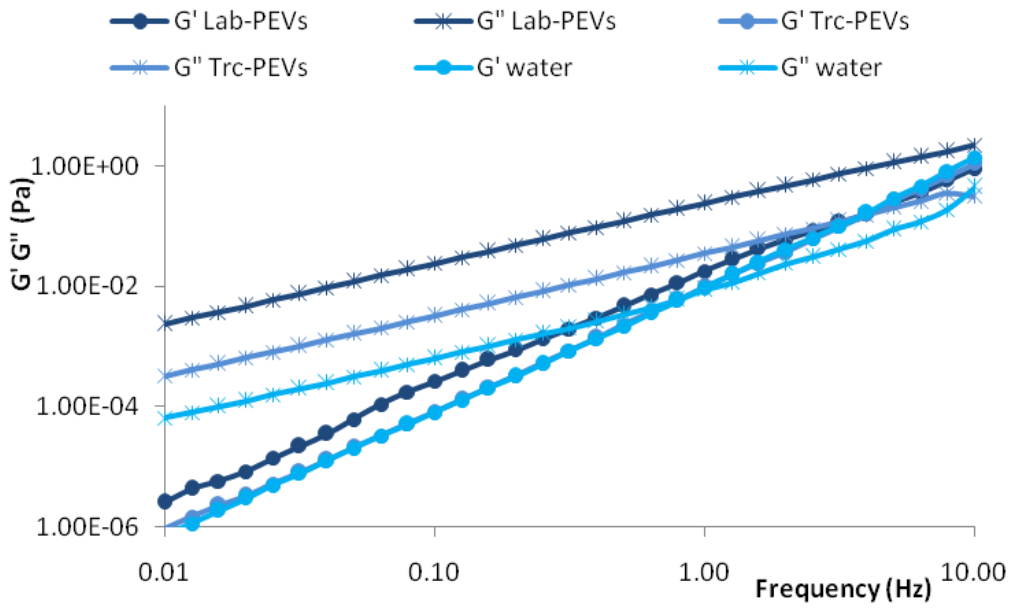

Figure 4. Determination of QUE deposition into pig skin layers (SC, stratum corneum; Ep, epidermis; D, dermis and RF, receptor fluid) after 8-h non-occlusive treatment: (a) QUE loaded in PEVs, (b) coarse dispersions of P50, PE

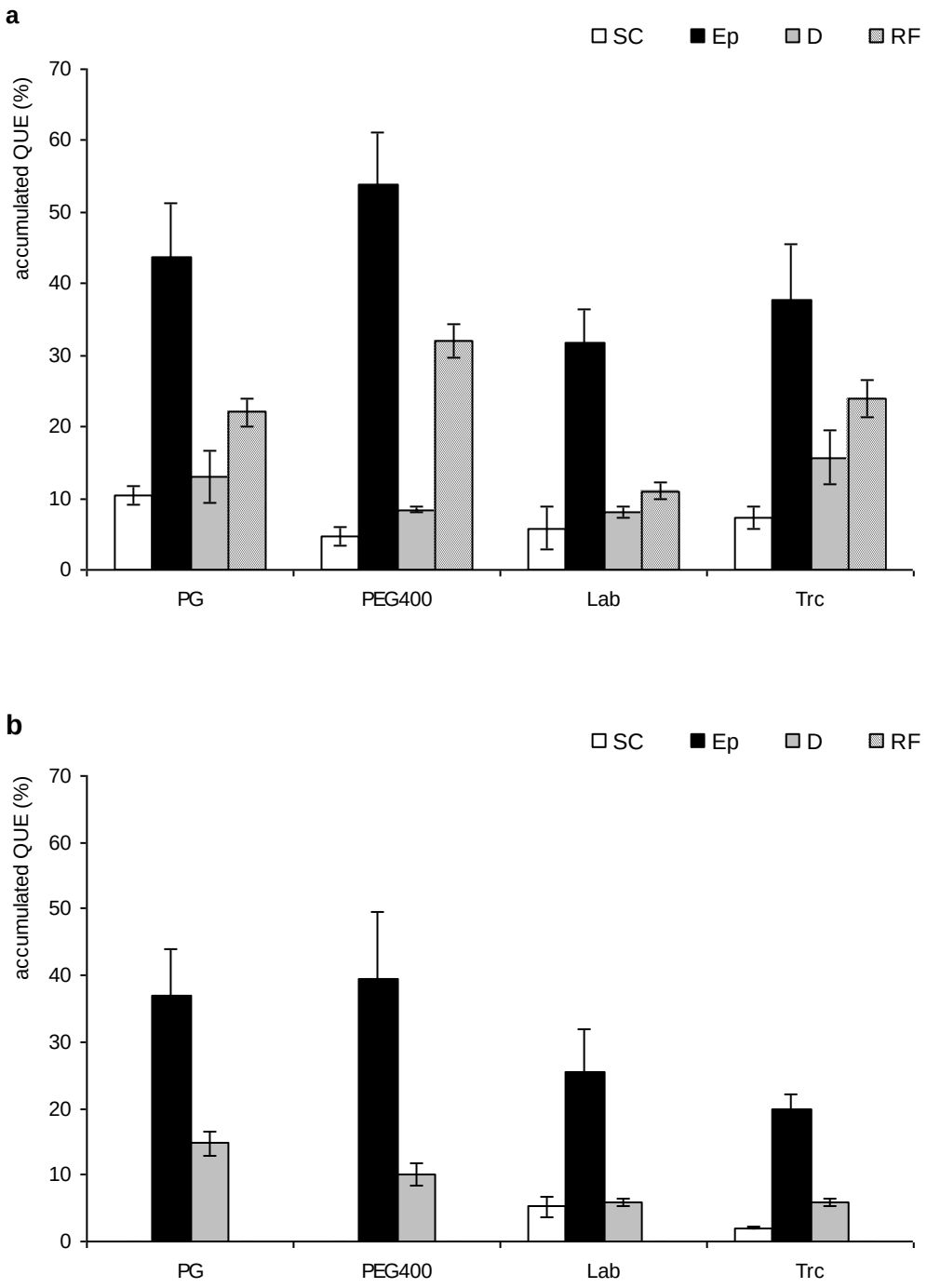

Figure 5. CLSM of cross-sections of new born pig skin treated for 8 hours with PEVs labelled with rhodamine-phosphoethanolamine. PG, PEG, Lab and Trc were used to formulate PEV dispersions**.**

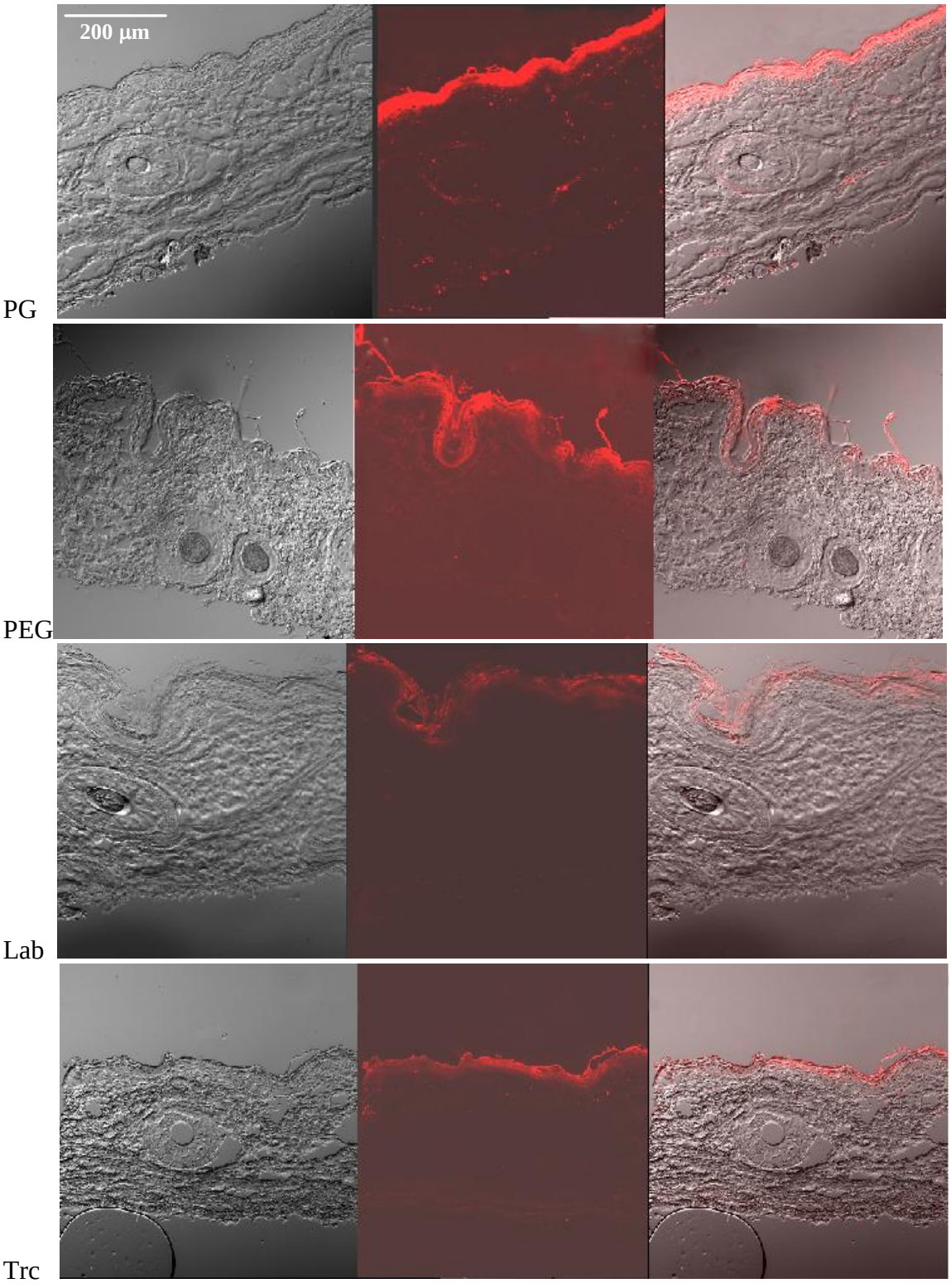

2.4. Conclusions

In this study we used a high amount (40%) of hydrophilic PEs to facilitate QUE incorporation into phospholipid bilayer, and to avoid QUE precipitation in vesicle dispersions. Results underline the ability of PEs (propylene glycol, polyethylene glycol 400, labrasol and transcutol) to improve drug solubility in vesicle dispersion, but above all, to have a synergic effect with phospholipids as penetration enhancers, which make PEVs potent nanocarriers for QUE skin delivery.

3.0. Development, characterization and ex vivo assessment of effective Penetration Enhancer containing Vesicles for dermal and deeper soft tissue delivery of phycocyanin on human skin

3.1. Introduction

Several studies have demonstrated the ability of topical fluid formulations to provide effective bioavailability of non-steroidal anti-inflammatory drugs (NSAIDs) in soft tissue pain and damaged skeletal muscle tissue higher than that obtained after oral administration, along with a lower plasma bioavailability (34, 35) Different drug carrier systems have been proposed for improving and prolonging the NSAID bioavailability in the skin and deeper tissues after topical application, such as liposomes, niosomes and transfersomes (36, 38). These systems are able to optimize dermal penetration and targeting of drugs (39, 41). As alternative vesicular systems, Penetration Enhancer containing Vesicles have been developed. They offer the advantage of associating the favorable properties of phospholipid vesicles and penetration enhancers (42, 50). In the present study phycocyanin-encapsulating PEVs (PC; 232 kDa),

an anti-inflammatory protein, have been formulated to facilitate local drug delivery to the skin and deeper soft tissues (subcutaneous adipose and skeletal muscle tissue), preventing systemic side effects of the drug. Phycobiliproteins are water-soluble and fluorescent proteins derived from cyanobacteria and eukaryotic algae. PC is one of the main biliprotein of blue-green algae, such as Spirula (Arthospira) maxima, used in pharmaceutical research as radical scavenger in oxidative stress-induced diseases and as strong antioxidant and anti-inflammatory (51). The antioxidant and anti-inflammatory properties of PC have been described by several authors (52, 55). Our previous studies showed that conventional phospholipid vesicles were capable of improving anti-inflammatory activity of PC in mice, in a dose dependent fashion. Indeed, liposomes were able to give the same anti-inflammatory response as the free protein by using half PC dose (55). In this work, PC was obtained from a dry extract (AfaMax®) of green blue microalgae Klamath (Aphanizomenon Flos Aquae). PC extraction and purity were confirmed by gel electrophoresis (SDS PAGE), MALDI top-down sequencing, LC/MS and UV absorption. Purified PC was encapsulated in different phospholipid vesicles. In particular, PEVs were prepared using a commercial mixture of phospholipids (Phospholipon 50, P50) and Transcutol® P (Trc) or propylene glycol (PG). Conventional phospholipid liposomes and ethosomes were prepared with the same phospholipid mixture P50, and used as controls. All vesicular dispersions were tested aiming at

evaluating the influence of the vesicular encapsulation on ex vivo PC penetration into and permeation through human skin. PC vesicles were labelled with rhodamine and their penetration extent and localization in the skin strata were examined by confocal laser scanning microscopy (CLSM). Moreover, fixed and sectioned tissue samples were visualized in three-dimensional structure using Scanning Electron Microscopy (SEM) to gain a complete picture of skin architecture and skin-vesicle interactions (46, 56).

3.2. Materials and Methods

3.2.1. Materials

Phospholipon® 50 (P50), a mixture of soy phospholipids (45% phosphatidylcholine and 10-18% phosphatidylethanolamine) was kindly supplied by AVG (Milan, Italy) and Lipoid GmbH (Ludwigshafen, Germany), and 1,2-dioleolyl-sn-glycero-3-phosphoethanolamine-N-(lissamine rhodamine B sulfonyl) (Rho-PE) was purchased by Lipoid GmbH (Ludwigshafen, Germany). Diethylene glycol monoethyl ether (Transcutol® P, Trc) was kindly provided by Gattefossè (Saint Priest, France). Ethanol (Et), propylene glycol (PG) and all the other products were of analytical grade and were purchased from Sigma-Aldrich (Milan, Italy). Phycocyanin (PC) was obtained from AfaMax®, an extract of AFA-phycocyanins from Klamath algae, from Nutratec (Urbino, Italy).

3.2.2. PC extraction and purification

PC was extracted from AfaMax® following the method by Benedetti et al. with some modifications (57). AfaMax® was dissolved in phosphate buffer saline (PBS, pH 7.4), brought to 50% saturation by the addition of ammonium sulfate, and allowed to stand for 60 minutes at 4 °C. The suspension was centrifuged (Heraeus Megafuge 1.0R) for 90 minutes at 40000 rpm and 4 °C to remove any insoluble material. The clear colourless supernatant was eliminated, and the blue precipitate was dissolved in a small volume of PBS and dialysed (Spectra/Por® tubing, 12–14 kDa MW cut-off; Spectrum Laboratories Inc., DG Breda, The Netherlands) overnight at 4 C against the same buffer. Dialysed PC was purified by gel chromatography with Sepharose® CL-4B pore size 60 – 20000 kDa (Sigma Aldrich, Milan, Italy), and the eluate lyophilized to obtain a blue powder to be loaded in vesicles, after the appropriate qualitative and quantitative testings.

3.2.3. SDS PAGE and in-gel digestion

The eluate from gel chromatography was separated on 15% sodium dodecyl sulphate polyacrylamide gels (SDS PAGE) using protein markers with a range of molecular weights from 10 to 250 kDa. Electrophoresis was run at 12 mA at room temperature, and the gel stained with Coomassie Brilliant Blue R-250 (Bio-Rad Laboratories, CA, USA). Bands of interest were cut from the gel and subjected to

enzymatic digestion with trypsin, according to Shevchenko et al.(58). The gel pieces were swollen in a digestion buffer containing 100 mM NH4HCO3 and 0.012 µg/µl in Ambic 10 mM of trypsin. After 45 minutes the supernatant was removed and discarded, 20 µl of 50 mM NH4HCO3 were added to the gel pieces and digestion allowed to proceed at 37 °C for 3 hours. The supernatant containing tryptic peptides was dried by vacuum centrifugation. Prior to mass spectrometric analysis, the peptide mixtures were redissolved in 10 µl of 5% formic acid.

3.2.4. Analysis of tryptic digested by LC-MS/MS

The obtained tryptic digests were analyzed according to LC-MS/MS, using a Q-TOF equipped with nano-spray source and analyzer hybrid quadrupole-time of flight, coupled to a chromatograph capillary UPLC equipped with a C18 column nano (Waters, Milan, Italy). The separation was conducted using water + 0.1% formic acid (eluent A) and acetonitrile + 0.1% formic acid (eluent B), and a linear gradient from 10 to 45% of B in 60 minutes, at a flow rate of 300 nl / min. Spectra were obtained in positive mode, over a range of m/z 500-1800. The ions of greater intensity were selected automatically by the instrument software and subjected to fragmentation within the collision cell (dependent scan analysis), producing MS/MS spectra information on the sequence of the peptides analyzed. The range of

m/z analyzed in both modes (MS and MS/MS) was calibrated using the fragment ions of the peptide Glu-Fib. The correction of the calibration takes place in real time using a system that injects Lock Mass Glu-Fib continuously during the analysis. For protein identification, the following parameters were used: complete carbamidomethylation of cysteines and partial oxidation of methionines, peptide mass tolerance ±1.2 Da, fragment mass tolerance ±0.9 Da, missed cleavages 2.

3.2.5. Peptide mass fingerprinting (PMF) by MALDI-TOF-MS

2 µl of the gel chromatography eluate containing the extracted protein were mixed with 2 µl of a matrix consisting of 1 mg of sinapinic acid dissolved in a mixture of distilled water and acetonitrile (1:1) plus 0.1% trifluoroacetic acid. Aliquots of 2 µl of protein solution-matrix were loaded onto a MALDI plate. Spectra were acquired using a MALDI-TOF mass spectrometer (micro MX, Waters, Milan, Italy). The sample was bombarded by a pulsed laser beam with $\lambda = 270$ nm, resulting in the production of ions. The analysis was conducted in positive mode, using a TOF linear in the range of m/z between 20000-170000 or between 2000-20000. The mass range analyzed was calibrated using an external standard mixture (2 µl) consisting of myoglobin [1 pmol/µl]: bovine serum albumin [1 pmol/µl] fortified with 1 µl of sinapinic acid in water:acetonitrile (30:70, v/v). Data were

acquired and processed by MassLynx software (Waters-Micromass). Protein identification was performed by searching in a nonredundant protein sequence database (NCBInr) using Mascot program (http://www.matrixscience.com), and results were considered significant if the resulting scores were higher than the threshold score indicated in the software.

3.2.6. Vesicle Preparation

Liposomes, ethosomes and PEVs were prepared using P50, Et, Trc or PG, empty or loaded with PC, as reported in Table 1. For liposomes and PEVs, all components were weighted in a glass vial, one after the other, and left hydrating for 2 hours in bidistilled water (59, 60). Then, the suspensions were sonicated (5 seconds on and 2 seconds off, 30 cycles) with a high intensity ultrasonic disintegrator (Soniprep 150, MSE Crowley, London, UK), until clear dispersions were obtained. For ethosomes, P50 and PC were dissolved in Et under mixing at 700 rpm. Bidistilled water was added slowly in a fine stream, under continuous stirring, in a well-sealed vial to avoid Et evaporation. The final suspension was sonicated as above.

All suspensions were prepared under yellow light and kept in the dark at all times.

3.2.7. Vesicle characterization

Vesicle dispersions were observed by a JEM1010 (Jeol Europe, Paris, France) transmission electron microscope (TEM) at 80 kV. The average diameter, polydispersity index (PI; a measure of the width of size distribution) and zeta potential of samples were determined by Dynamic and Electrophoretic Light Scattering using a Zetasizer nano-ZS (Malvern Instruments, Worcestershire, UK). Samples diluted (1:100) in water or Trc/, PG/, Et/water mixtures at the same ratio used for vesicle preparation, were analysed 24 hours after their preparation, at a constant temperature of 25 °C. Vesicles were separated from the non-encapsulated drug by exhaustive dialysis: dispersions were loaded into dialysis tubing (300 kDa Float-A-Lyzer® G2, Spectrum Laboratories Inc., DG Breda, The Netherlands) and dialysed against water or PE/water mixture for 2 hours at 25 °C, which was appropriate to allow the dissolution and consequent removal of the non-encapsulated PC. Drug content and vesicle loading efficiency (E%), expressed as the percentage of the amount of drug initially used, were determined using a UV-visible spectrophotometer (Lambda25, Perkin Elmer, Monza, Italy) at 615 nm.

3.2.8. X-ray diffraction

Vesicle structure was studied by Small and Wide-Angle X-ray Scattering (SWAXS). SAXS and WAXS patterns were recorded

simultaneously using a S3-MICRO (Hecus X-ray systems, Graz, Austria) coupled to a GENIX-Fox 3D X-ray source (Xenocs, Grenoble, France) working at 50 Kv and 1 mA. This source produces a focused X-ray beam with λ=1.542 Å at Cu Kα-line with more than 97% purity and less than 0.3% Kβ. The two detectors are position sensitive detectors PSD 50 (Hecus, Graz, Austria). The working q-range were $0.01 \leq q \leq 0.6$ Å−1, in the small angle, and $2.8 \leq q \leq 3.5$ Å−1 in the wide angle range, where $q = (4 \pi \sin \theta)/\lambda$ is the modulus of the scattering wave vector, θ the scattering angle and λ the wavelength. Vesicular dispersions were loaded into thin-walled 1 mm glass capillaries for the scattering experiments. The diffraction patterns were recorded at 25 °C. All scattering curves were reproduced twice with subsequent calculation of the electron distance distribution, and yielded identical results. For the figures, a representative curve was selected, plotting the scattering intensity I as a function of the scattering vector q. SAXS patterns were analyzed using the MCG model developed by Pabst et al.(61). The analysis technique models the full q-range in the SAXS regime, including Bragg peaks and diffuse scattering. The bilayer electronic density profile is calculated as the sum of three gaussians, one corresponding to the methyl contributions and the other two corresponding to the polar heads. As a difference with respect to the model of Pabst et al. (61) we also incorporated a constant term through the hydrophobic part of the bilayer to give account for the methylene contribution. The

interbilayer ordering is taken into account considering the modified Caillé model as in the work by Pabst et al.(61). By this procedure, relevant structural parameters, as well as the distribution of electron density in the polar and apolar regions of membranes, were obtained. The model allowed fitting the SAXS pattern of bilayer-based structures, i.e. vesicles and lamellar phases. From the analysis, the membrane thickness was obtained through the definition dB = 2 (Zh + fwhm / 2), where Zh is the distance to the center of the bilayer of the polar head Gaussian with the corresponding full-width at half maximum fwhm. To derive the other parameters, we used 158.5 electrons for the polar head and 261.9 electrons for the hydrophobic tails (based on the composition of P50).

3.2.9. Confocal Laser Scanning Microscopy (CLSM)

Vesicles were labelled by adding Rho-PE to the phospholipid mixture. The penetration extent and distribution of fluorescent PC in rhodamine-labelled vesicles was investigated ex vivo through full-thickness human skin obtained from patients undergoing abdominal plastic surgery. The labelled colloidal dispersions (100 µl) were applied onto the skin (n = 6 per formulation) mounted on Franz vertical cells (diffusion area 0.785 cm2). Experiments were carried out in non-occlusive conditions, for 8 hours. After that, skin specimens were gently washed with distilled water, the diffusion area punched

out and rapidly frozen at -80 °C. Sections of skin (7 μm thickness) were cut with a cryostat (Leica CM1950, Barcelona, Spain) orthogonally (in the z axis) to the surface, and examined under a FluoView FV1000 inverted confocal microscope (Olympus, Barcelona, Spain) equipped with a Ultraviolet/Visible light laser. Using a UPlanSApo 20x objective NA 0.75, images with a field size of 1024 × 1024 μm were generated. PC and rhodamine were excited at 600 nm and 559 nm, and detected at 640 nm and 578 nm, respectively.

3.3.0. Scanning Electron Microscopy (SEM)

At the end of Franz experiments (as above), skin specimens were gently washed, the treated area punched out, immediately immersed in PBS 0.2 M, pH 7.3, and fixed with Karnovsky's paraformaldehyde-glutaraldehyde solution. After fixation, samples were dehydrated in graded ethanolic solutions (30, 50, 70, 96 and 100%, v/v), subjected to critical point drying, and coated with gold to prevent sample charging. Samples were visualized under a scanning electron microscope (SEM) Hitachi S4800 (Madrid, Spain).

3.3.1. Statistical analysis of data

Data analysis was carried out with the software package R, version 2.10.1. Results are expressed as the mean ± standard deviation (SD).

Multiple comparisons of means (Tukey test) were used to substantiate statistical differences between groups, while Student's t-test was used for comparison between two samples. Significance was tested at the 0.05 level of probability (p).

3.4. Results and discussion

The complete purification of PC from microalgae biomass is a complex procedure resulting in a very expensive commercial product (62). To obtain a suitable product available for pharmaceutical purposes, we extracted PC from AfaMax® simplifying the method by Benedetti et al. (57). for an efficient separation and purification of the protein. We obtained 40% yield (w/w) of PC from AfaMax® extract. UV-visible spectrophotometric reading of the extracted protein, in comparison with commercial PC (C-PC from Spirulina sp.; Sigma-Aldrich, Milan, Italy), and SDS-PAGE analysis were performed to evaluate the purity and content of PC in the extract. Two main bands of purified PC were visible in SDS-PAGE under reduced conditions, corresponding to α and β subunits with the predicted molecular weights of about 18 and 19 kDa, respectively (Figure 1). Furthermore, the UV-visible spectrum revealed the characteristic absorption band of PC at λmax 620 nm (data not shown). The identification of α and β subunits separated by SDS–PAGE was also confirmed using MALDI mass spectrometry.

Figure 1. SDS PAGE analysis (A) and MALDI-TOF spectrum (B) of purified phycocyanin from AfaMax® extract.

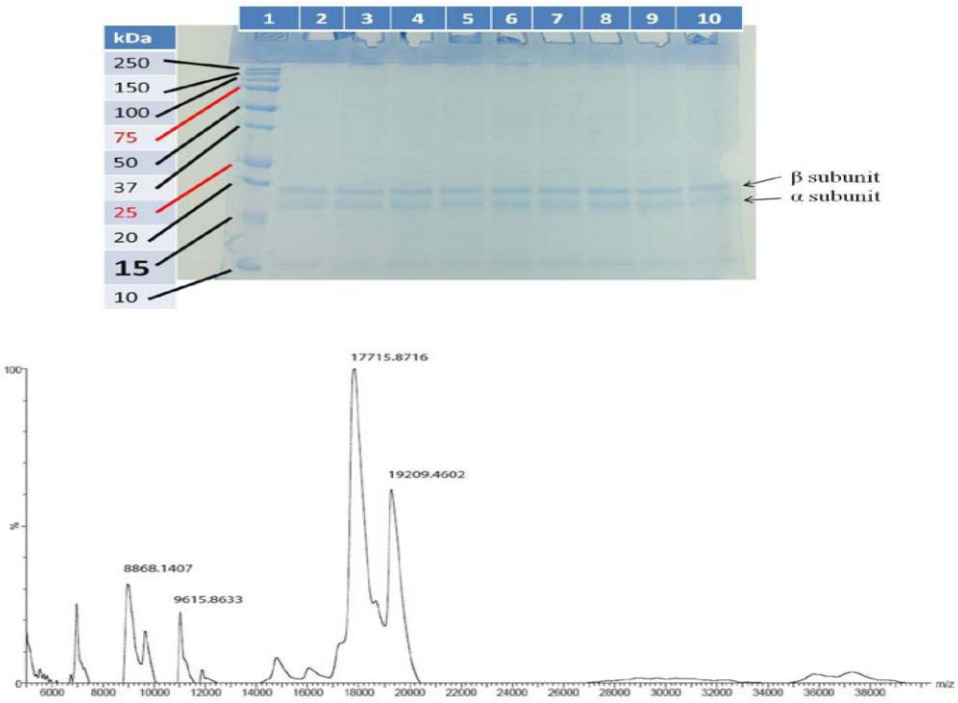

The representative MALDI-MS spectrum recorded is displayed in Figure 1, where two main peaks identifiable as α- and β-PC subunits were detected (m/z 17715.8716 and 19209.4602, respectively). Moreover, in the low m/z region of the spectrum, the corresponding doubly charged ions were also present. Tryptic digestion of proteins contained in the SDS-PAGE bands led to consolidate the protein

identification by PMF using MALDI-TOF and/or by Peptide fragment fingerprinting (PFF) using nano-LC/MS/MS. Specific m/z values were obtained for each protein band and the corresponding MS/MS data to confirm the protein. Both Mascot and Protein prospectors were used as search engines. The gel band at 18 kDa was successfully attributed to the α PC subunit. Eight specific m/z values used in protein search were compatible with tryptic peptides from this protein (mass accuracy between 1 and 15 ppm), obtaining a sequence coverage of 70%. These data permitted an unambiguous identification of α PC subunit. The second band at 19 kDa was successfully attributed to the β PC subunit. Fourteen specific m/z values used in protein search were compatible with tryptic peptides from this protein (mass accuracy between 1 and 15 ppm), obtaining a sequence coverage of 71%. Thus, unambiguous identification of the β PC subunit was obtained. Our results are in conformity with previous reports on the α and β subunits of PC from blue-green algae (63, 65). Altogether these results indicate a ~ 90% purity of PC in the purified blue powder obtained from AfaMax® extract.Once the protein was successfully extracted, purified and identified, it was encapsulated in different vesicular nanocarriers: liposomes, ethosomes and PEVs, prepared by direct sonication, without the use of any organic solvents. Sample composition is reported in Table 1.

Table 1. Composition of vesicular dispersions.

Components	Liposomes	Trc-PEVs	PG-PEVs	Ethosomes
P50	60 mg	60 mg	60 mg	60 mg
PC	10 mg	10 mg	10 mg	10 mg
Trc		0.2 ml		
PG			0.2 ml	
Et				0.2 ml
water	1 ml	0.8 ml	0.8 ml	0.8 ml

Table 2. Properties of P50 vesicles: mean diameter, polydispersity index (PI), and zeta potential (ZP). Values are the means ± standard deviation (n =6).

		Size (nm ± SD)	PI	ZP (mV ± SD)
Liposomes	**Empty**	64±3	0.21	-63±2
	PC	124±5	0.22	-39±2
Trc-PEVs	**Empty**	67±3	0.20	-45±2
	PC	187±4	0.27	-27±5
PG-PEVs	**Empty**	60±4	0.26	-45±2
	PC	177±6	0.26	-24±3
Ethosomes	**Empty**	61±2	0.25	-54±4
	PC	142±7	0.29	-26±6

Characteristic parameters of vesicle formulations are summarized in Table 2.

Empty vesicles were always smaller than the corresponding protein-encapsulated ones, probably because the large PC molecule interacts with bilayer polar regions increasing its curvature and, consequently, the size. Further, it was apparent that, in empty vesicles, the presence of the PE did not alter vesicle size, whereas PC conventional liposomes showed the smallest mean diameter ($p < 0.05$). The mean size of vesicles increased slightly using Et, and more significantly using Trc and PG, probably because PC interacts with bilayer surface increasing its curvature and these PC-phospholipid polar head interactions are modulated by PE polarity. Zeta potential values were similar for all empty PEVs (~ -47 mV) and became more negative for empty liposomes (-63 mV), showing a negative surface charge due to P50 anionic lipidic fractions (49, 66). It has to be noted that the PC loading of vesicles resulted in less negative zeta potential values, because at a pH (~ 5) below its isoelectric point (pI ~5.8), PC carries a net positive charge.

Dialysed vesicles showed slightly larger size than the corresponding non-dialysed samples (data not reported). As known, dialysis can induce an increase in vesicle size as a consequence of the osmotic stress during this purification procedure. However, the increase was not statistically significant.

All P50 vesicles were able to incorporate an acceptable amount of PC (around 40%), without statistical differences among the various formulations. Indeed, the PEs did not affect E%. PC is a large hydrosoluble molecule that is present at the same concentration in the internal and external medium of vesicles. Thus, the amount of encapsulated PC depends on the volume of vesicle aqueous compartment, which is usually low, and consequently E% (67). The presence of PE did not change the drug solubility and then, the amount of encapsulated drug.

A preliminary investigation on vesicle formation and morphology was carried out by TEM (Figure 2).

Figure 2. Phycocyanin-encapsulated liposomes **(A)** and Trc-PEVs **(B)**.

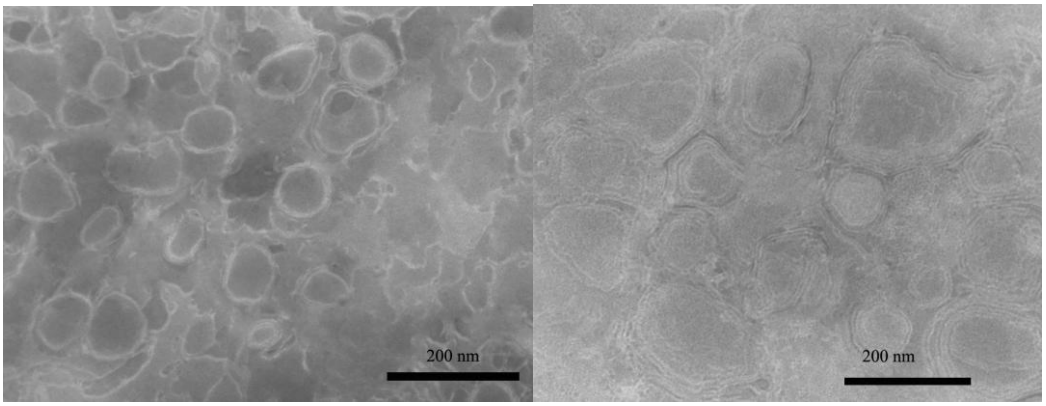

Liposomes were spherical and unilamellar, while PEVs showed more irregular shape, in particular PG-PEVs (44), as previously reported for diclofenac PG-PEVs (46). On the other hand, Trc-PEVs appeared multilamellar.

To gain further information about salient features of the prepared vesicular systems regarding their geometrical properties and morphology, SAXS and WAXS were used, as they are among the principle techniques for the microscopic characterization of self-assembling structures in the nanometer scale. SAXS experimental data was fitted to a bilayer model with interbilayer correlations (see the experimental part for further details). In Figure 3 the resulting fits are shown as lines. The reduced chi square ($\chi 2 = 1$ for purely statistical noise) values were below 2 (nearly perfect fitting), except for the samples containing Trc where it was around 10. However, the quality of these fits was still quite good.

Figure 3. Small angle X-ray diffraction patterns (SAXS) of liposomes, ethosomes and PEVs. For the sake of clarity the curves of empty liposomes and ethosomes have been omitted, as superimposable to the corresponding phycocyanin (PC) loaded vesicles.

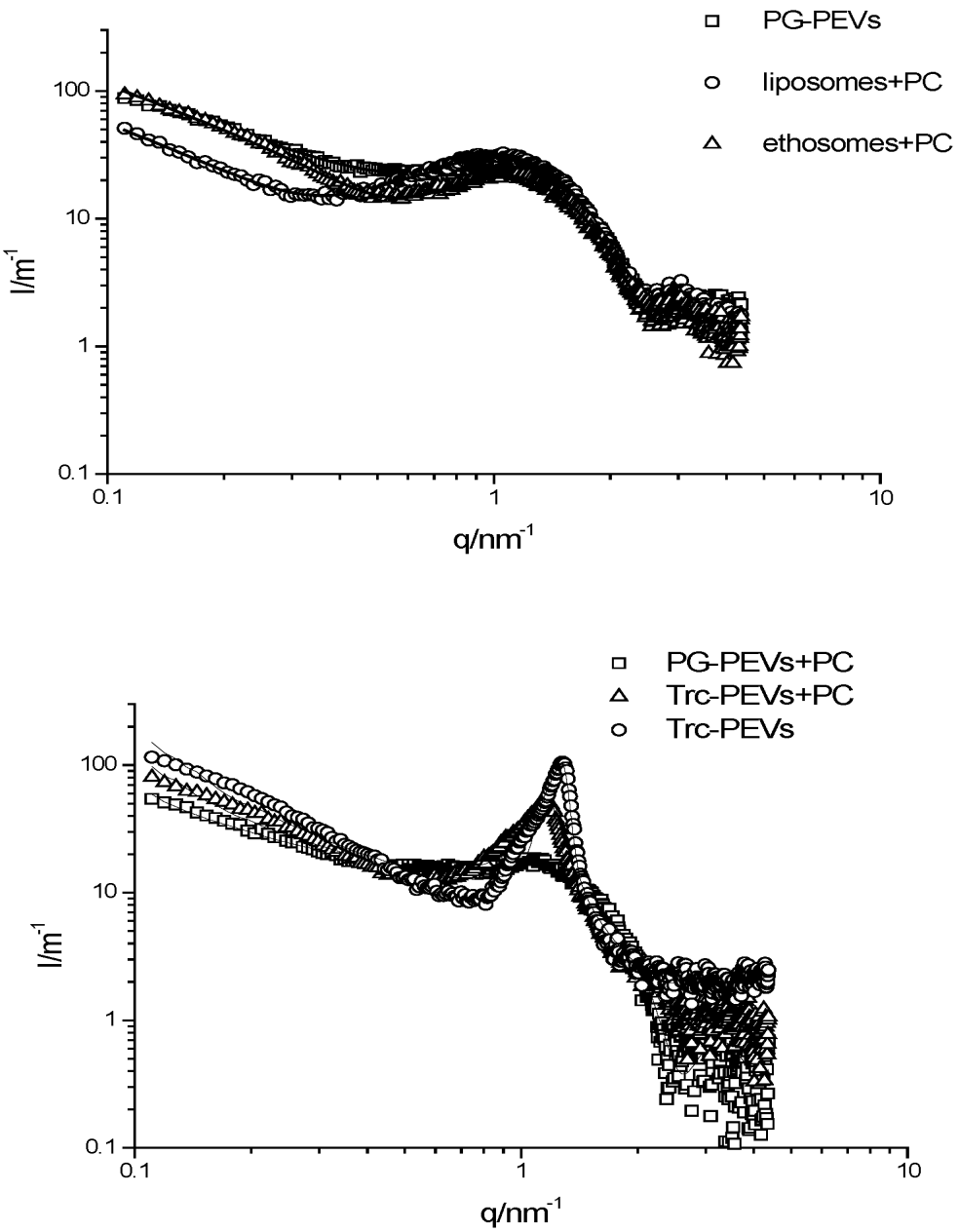

Table 3. Selected fitting parameters and derived parameters for SAXS curves. All distances are given in nm.

	Liposomes +PC	Ethosomes +PC	PG-PEVs +PC	Trc-PEVs +PC
[1] **d**	5.04±0.5	4.51±0.5	4.93±0.1	5.19±0.05
[2] **η**	1.82±0.2	1.38±0.2	1.15±0.2	0.46±0.05
[3] **N**	2.7±0.3	2.5±0.3	14.0±2	35.1±5
[4] **σ_h**	0.33±0.005	0.28±0.005	0.21±0.005	0.32±0.01
[5] **Z_h**	1.83±0.01	1.72±0.01	1.77±0.01	1.73±0.05
[6] **d_c**	1.44±0.02	1.39±0.02	1.52±0.02	1.36±0.06
[7] **d_B**	4.46±0.04	4.10±0.04	4.04±0.04	4.22±0.13
[8] **d_w**	0.58±0.5	0.40±0.5	0.89±0.1	0.98±0.05

[1] d repetition distance; [2] η Caillé parameter; [3] N number of correlated lamellae; [4] σ_h polar head amplitude; [5] Z_h polar head distance to the center of the bilayer; [6] d_c hydrophobic chains layer half-thickness; [7] d_B bilayer thickness; [8] d_w water layer thickness.

As evident from the SAXS pattern, showing a diffuse scattering with broad symmetric band, empty liposomes, ethosomes and PG-PEVs can be considered unilamellar. The addition of PC slightly modified the scattering curves, but the derived parameters for the bilayer were

very close. This was not true in the presence of PG. Indeed, PG-PEVs loading PC showed a correlation, even though the uncorrelated bilayers were predominant, thus indicating the presence of a mixed population of multilamellar and unilamellar vesicles. On the other hand, Trc-PEVs showed stronger correlation, typical of multilamellar vesicles. The diffraction intensity decreased due to the decrease in the number of layers induced by PC presence.

In the case of empty liposomes, ethosomes and PG-PEVs, none of the penetration enhancers noticeably affected bilayers features and correlated parameters. They were unilamellar, soft vesicles with low number of correlated layers ($N \sim 2$), the Caillé parameter $\eta \sim 1.6$, and bilayer thickness $dB \sim 4.2$ nm. Additionally, they did not perturb strongly Zh (~1.7), that is, the separation between the polar heads and the center of the bilayer. It is noteworthy that the loading of PC did not alter the above parameters for liposomes and ethosomes. In contrast, a strong effect was observed with Trc (Zh = 1.88), which converted the vesicles in relatively stiff multilamellar vesicles (decrease in Caillé parameter, $\eta = 0.16$, and high number of correlated layers, $N = 20.5$). The additional presence of PC seemed to slightly reduce the stiffness of Trc-PEVs bilayers (Figure 3 and Table 3). This is in good agreement with TEM analyses, where Trc-PEVs were seen as multilamellar (Figure 2B). Regarding PG-PEVs loading PC, the simultaneous presence of PG and PC caused a partial multilamellarity,

implying a certain stiffness, as also confirmed by a high N value (=14).

The presence of Trc and PG in combination with PC, determined an increase in vesicle size and lamellarity that corresponded to a stiffening of the bilayers. This was not true for Et that gave larger vesicles but still unilamellar, thus confirming the soft and malleable nature of ethosomes (68) In addition, the multilamellarity of Trc-PEVs and PG-PEVs (partial) loading PC was reflected in the interbilayer water thickness dw, which was almost 2-fold higher than liposomes and ethosomes. Lamellar Bragg distances (d; Table 3) were all around 5.0 nm for both empty and loaded samples. Concerning multilamellar Trc-PEVs, the addition of PC seemed to increase the interlamellar distance. This increase was accompanied by a strong increase in the hydration of the polar heads (σh = 0.32 vs 0.22 for empty vesicles). The addition of PC also produced an appreciable reduction in the hydrophobic bilayer thickness (dc = 1.36 vs 1.62 for empty vesicles; also reflected in the decrease in Zh). However, the total bilayer thickness dB remained almost unchanged, due to the increase in the polar head region, σh. This is in accordance with the nature of PC locating mainly in the polar head region of the bilayers.

Overall, from Table 3 it can be inferred that the simultaneous presence of PEs and PC caused a decrease in the bilayer thickness dB, mostly due to a decrease in the hydration of the polar heads (compare σh of liposomes vs the other vesicular systems), correlated to a predominant

interaction of hydrophilic PEs and PC with the polar region of bilayers. As expected, the SAXS spectra did not show any distinct peaks for non-organized structures in this range of distances, indicative of liquid-crystalline state (Lα). However, the electronic density profiles (data not shown) could be compatible with partial segregation of the terminal methyl groups in the case of ethosomes and PG-PEVs loading PC.

In our previous work, liposomes were capable of improving in vivo anti-inflammatory activity of PC in a dose-dependent fashion, as a consequence of enhanced PC skin delivery obtained using liposomal carriers (55). Our further studies, suggest that PEVs possess a superior ability to improve dermal deposition and transdermal permeation, with respect to conventional liposomes (44, 49). Indeed, drug penetration through the skin depends strongly on its physicochemical properties and on the carrier in which it is applied. In ethosomes and PEVs, the presence of the water cosolvent, influences both the vesicle properties and the barrier function efficacy of the skin, facilitating the active compound passage and accumulation into the skin (68, 69). In the present study, a CLSM study was carried out to evaluate the vesicle formulations' ability to allow PC penetration and distribution through human skin. The skin was observed microscopically after 8 hours of ex vivo treatment with fluorescent PC-loaded rhodamine-labelled vesicles. Images of the skin treated with empty vesicles did not reveal any fluorescence signal, and skin autofluorescence was not detected.

Figure 4. Cross-sectional images obtained following treatment with phycocyanin-encapsulating liposomes, ethosomes, PG-PEVs and Trc-PEVs.

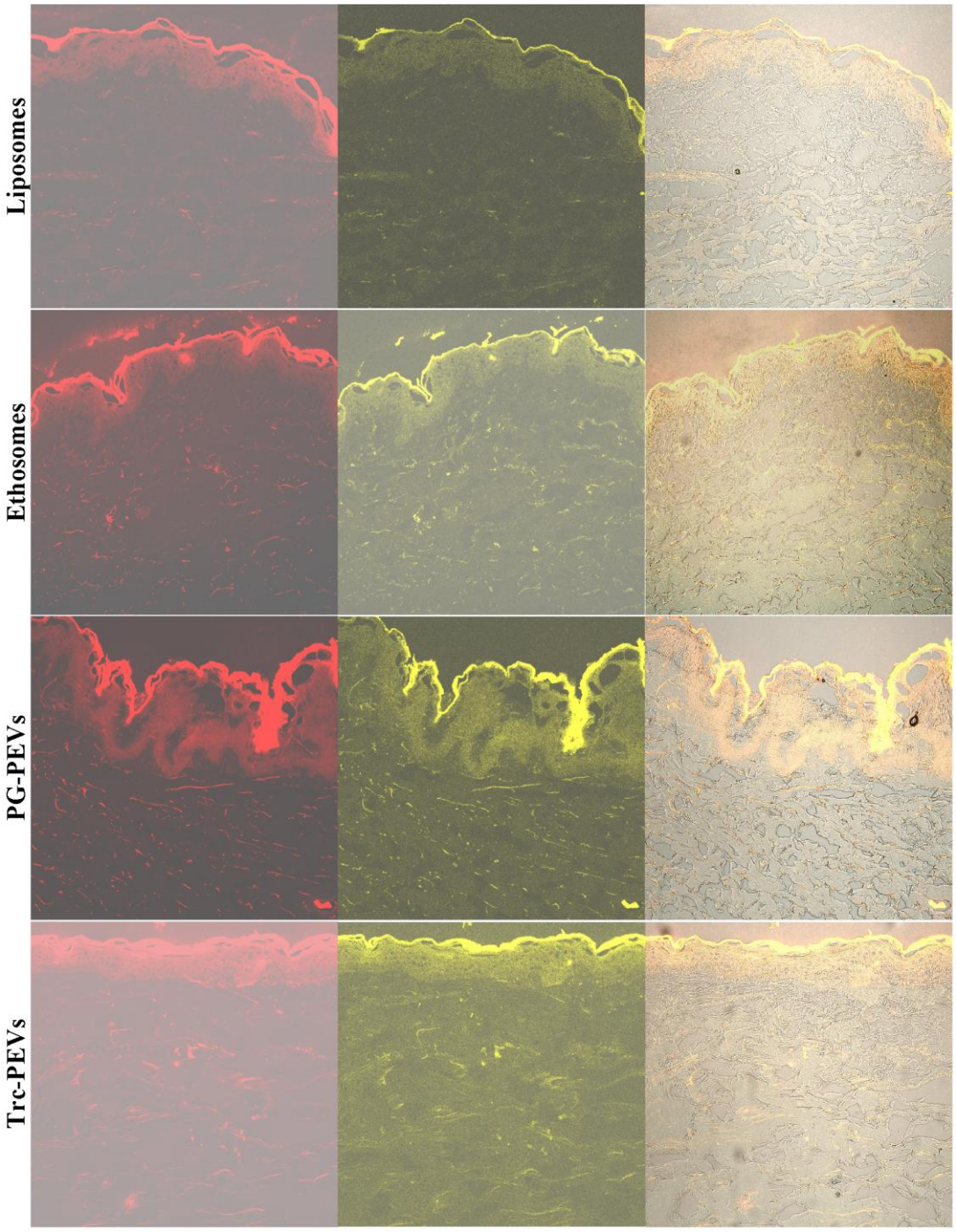

Figure 4 consists of four representative, optical cross-sections, selected from several images and several different zones of treated skin. In the lefthand, we reported rhodamine fluorecence (red), in the middle PC florescence (yellow) and in the righthand the merge of the two probes' fluorescence: the orange color shows the probes' superposition. The observed fluorescence accumulation across the stratum corneum and viable epidermis was relatively homogeneous in all the tested formulations, and was higher than that observed in the dermis that exhibited a less intense and diffuse staining. Images indicate that all vesicles were able to deliver the protein deeply to the skin. In particular, PEVs showed a penetration ability greater than liposomes and ethosomes, which presented a dominating staining in the stratum corneum, as compared to that in the viable epidermis. The dual image analysis by the probe colocalization provides a clear illustration of the possible vesicle distribution (orange fluorescence). These results indicate that PEVs, especially PG-containing vesicles, are promising carriers for the delivery of the high MW PC molecule to the deep skin layers, where its anti-inflammatory activity needs to be exerted.

In order to better evaluate the vesicle-skin interaction, we observed immobilized skin by SEM (48, 58) Images visualize the immobilized tissue in three-dimensional form (Figure 5).

Figure 5. SEM images of untreated (a) and liposome- (b), ethosome- (c) and PEV- (d) treated skin

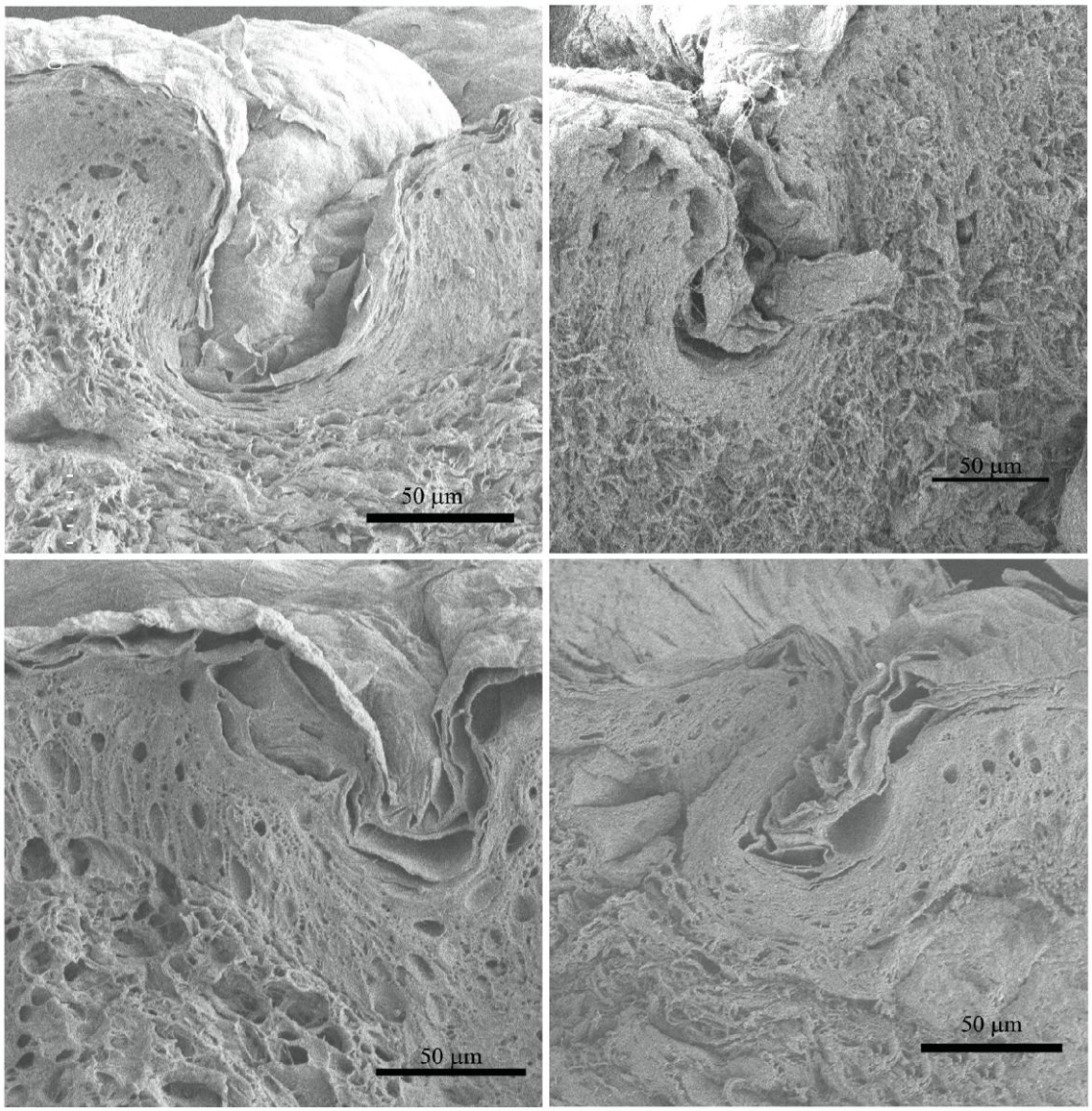

Untreated human skin tissue was first imaged as a control. The epidermis ultrastructure of the untreated tissue appeared compact and thin, whereas following application of different PC vesicles, skin

appeared swollen. In particular, skin treated with PEVs showed evident intercellular spaces of the stratum corneum indicating a high hydration. There is a 10–20% increase in thickness of the SC. Hydration is known to improve the skin permeability and could enhance penetration of macromolecules, such as proteins. A 4-10-h hydration period is enough to enhance transcutaneous penetration of large biomacromolecules without permanently damaging the skin (71). SEM images validated our hypothesis regarding the mechanism of PEV-skin interactions: PEVs, thanks to a synergic effect of PE and phospholipid vesicles, partially penetrate intact until the epidermis and partially fuse with the intercorneocyte lamellar structure of stratum corneum hydrating it.

3.5. Conclusion

PC is a natural biliprotein with important anti-inflammatory and anti-oxidant activities, but its use in pharmaceutical applications is limited by its high cost. Results of this work confirmed the feasibility of obtaining from a commercial extract a product suitable for pharmaceutical uses, with 90% of purity degree. The encapsulation of extracted PC into PEVs, especially PG-PEVs, facilitated the accumulation of the high molecular weight drug into the deep skin layers where drug needs to exert its action. Thanks to their innovative formulation containing a PE into vesicle structure, PEVs can act

simultaneously as penetration enhancers and carriers facilitating the (trans)dermal delivery of PC protein.

Acknowledgements and Funding

Sardegna Ricerche Scientific Park (Pula, CA, Italy) is acknowledged for free access to facilities of the Nanobiotechnology Laboratory. Dr. C. Caddeo was financed by Regione Autonoma della Sardegna under the POR Sardegna FSE 2007/2013.

4.0 Respiratory system

In the last year of my PhD thesis I started a new formulation study in Paris, Université Paris Sud XI, Chatenay-Malabry. During this period I prepared and characterized new hybrid lipid-polysaccharide nanocarriers for curcumin pulmonary delivery composed of curcumin loaded-liposomes modified with chitosan. Liposomes, as pulmonary drug delivery carriers, have been studied for years and used to deliver phospholipids to the alveolar surface for the treatment of lung disease and systemic diseases. Inhaled liposomes reach the alveoli, achieving a prolonged pulmonary retention time of drug and increasing the efficacy of drug in vivo (72-74). Moreover, phospholipids are absolutely biocompatibile and have also beneficial effects for lung surfactants, often compromised during this disease. Thus, liposomes protect encapsulated curcumin from external environment and have the advantage of vehiculating the poor soluble curcumin in an aqueous environment with a consequent enhanced bioavailability. Liposome surface was coated with chitosan in order to improve liposome stability, and mucoadhesion (75-77). In fact, chitosan is a polycationic polysaccharide that possesses promising properties in drug delivery, such as biocompatibility and biodegradability that make it an attractive vehicle for designing adequate dosage forms for pulmonary drug delivery. Moreover, chitosan is a bioadhesive polymer that could avoid curcumin-liposome clearance by the mucociliary escalator. Curcumin, useful to limit cystic fibrosis pulmonary disease

progression, can be pulmonary delivered by using chitosan coated liposomes.

Pulmonary administration of drugs, in the treatment of localized diseases within the bronchi, allows to delivery high amount of the drug into the diseased regions. The highly efficient clearance of mechanisms of the human respiratory tract causes a fast drug action after dosing. Therefore, an adequate carrier vehicle may facilitate the drug transport to the lung, prolonging its retention time in the epithelia tissue, avoiding its degradation at pH 7.4, and improving its local absorption, thus maintaining therapeutic concentrations of the drug within the lung tissues.

5.0. Chitosomes as drug delivery system for curcumin pulmonary administration

5.1. Introduction

Cystic fibrosis is chronic, progressive, and usually fatal disease caused by defective function of a gene product, Cystic Fibrosis Transmembrane Conductance Regulator (CFTR). Cystic fibrosis is characterized by abnormal chloride transoport in many tissues, including lung, pancreas, gastrointestinal tract, liver, sweat glands, and male reproductive ducts (78).

Current therapeutic approaches to pulmonary cystic fibrosis primarily focus on restoring the function of the CFTR, stimulating alternative chloride channels, inhibiting sodium absorption, and utilizing hyperosmotic agents to rehydrate the airway surface. An approach to rescue CFTR function in the airways epithelia is corrects the defects associated with mutant CFTR proteins or alternatively enhance the function of the CFTR chloride channel (79).

Curcumin (1,7-bis(4-hydroxy-3-methoxyphenyl)-1,6-heptadiene-3,5-dione) is a non-toxic bioflavonoid that have antioxidant activity, and inhibits such mediators of inflammation as NFκB, cyclooxygenase-2, lipooxygenase, and inducible nitric oxide synthase. Curcumin are able to rescue mutant gene (ΔF508) CFTR in airway epithelial cells and

mouse models. Although other studies have underlined that curcumin can produce an increase in CFTR channel activity. Its action mechanism is controverts but it is actually able to stop cystic fibrosis pulmonary disease progression thank to its ability to enhance CFTR channel function synergically to its antioxidant and antinflammatory activity.

In this work, aiming at improving curcumin solubility and its time retention into lung tissue, a novel plymer surface-modified liposome formulation was designed. In fact, liposomes thanks to their are high biodegradable and biocompatible are a suitable lung delivery system that offer advantages of local administration, uniform deposition and high surface distribution of active drug. Liposomes coated with suitable polymers can improve drug bioadhesion, modify pharmacokinetics, and protect the encapsulated drug from enzymatic attack. Among the various polymers, able to interact with liposome surface chitosan (CH) possess good mucoadhesive properties and are able to their protect and stabilize. Moreover, it has already successfully used to coat liposome formulations (80). Surface modification of liposomes with CH has been shown to prolong their residence time in the airways in comparison with uncoated ones, thanks to ionic interactions between positive amino groups of the polymer and the negative mucus gel layer (81).

Liposomes formulations were prepared using a mixture of soy lipids (Phospholipon 50, P50) and curcumin and they were used as control.

Liposomes surface were then coated by adding chitosan to control formulation. Prepared vesicles were thoroughly characterized by size, surface charge and loading and aggregation capacity. The in vitro cytotoxicity, cellular uptake, induced by the different liposomes were all assessed using the Calu-3-based model of lung epithelium (82).

5.2.Materials and Methods

5.2.1. Materials

A commercial mixture of soybean phospholipids (Phospholipon® 50, P50, with 45% phosphatidylcholine and 10-18% phosphatidylethanolamine, maximum 3% triglycerides, maximum 0.25% D,L-a-tocopherol, and the remaining part (37%) lipids: fatty acids, glycolipids, phosphatidylinositol, etc) was kindly supplied by AVG (Milan, Italy) and Lipoid GmbH (Ludwigshafen, Germany). 1,2-dioleoyl-sn-glycero-3-phosphoethanolamine-N-(lissamine rhodamine B sulfonyl) ammonium salt (rhodamine-phosphoethanolamine, Rho-PE) was purchased from Lipoid GmbH (Ludwigshafen, Germany). Chitosan (CH) low molecular weight, curcumin (CUR) (1,7-bis(4-hydroxy-3-methoxyphenyl)-1,6-heptadiene-3,5-dione) and all others products were purchased from Sigma (Milan, Italy).

5.2.2. Liposome preparation

Curcumin (5 mg/ml) was dispersed in the water and added to the flask containing P50 (60 mg/ml). Lipids were left swelling in the solution overnight (62) and sonicated for 2 minutes (5 seconds on and 2 seconds off) using a Soniprep 150 ultrasonic disintegrator (MSE Crowley, United Kingdom).

Each vesicle suspension was purified from the non-incorporated drug by dialysis against distilled water at 4°C for 4 hour, using dialysis tubing (Spectra/Por® membranes: 12–14 kDa MW cut-off, 3 nm pore size; Spectrum Laboratories Inc., Ranchio Domingo, USA).

Liposome formulation (5 ml) was diluited in distiled water (10 ml) to obtain the same drug concentration of chitosomes.

5.2.3. Chitosome preparation

Appropriate amount of chitosan (50 mg/ml) was dissolved under stirring in acetic acid (0.1%) aqueous solution. Dyalised CUR loaded liposomes (5 mL) were slowly added to the CH dispersion (10 mL) under stirring at 25°C to obtain the final chitosomes. Dispersions were ultracentrifuged at 40000 RPM for 4 h at 4°C to eliminate the excess of chitosan and washed three times with distilled water.

Table 1. Composition of curcumin liposomes and chitosomes

	CUR (mg/mL)	P50 (mg/mL)	CH 0.5% (mg/mL)
Liposomes	1.7	20	-
Chitosomes	1.7	20	3.3

5.2.4. Liposomes and chitosome charaterisetion

Formation and morphology of vesicles and chitosomes were evaluated by Transmission Electron Microscopy (TEM) using a JEOL JEM-1400 microscope (CNRS, Gif s/Yvette, France) operating at 80kV. Average diameter and polydispersity index (PI) of the samples was determined by photon correlation spectroscopy using a Zetasizer nano (Malvern Instrument, Worcestershire, United Kingdom). Before counting, the samples were diluited with distilled water. Samples were backscattered by helium–neon laser (633 nm) at an angle of 173° and at constant temperature of 25°C. Zeta potential was estimated using the Zetasizer nano by means of the M3-PALS (phase analysis light scattering) technique, which measures the particle electrophoretic mobility in a thermostated cell. All the samples were analyzed 24 h after their preparation.

Quantitative determination of phospholipids was carried out using an enzymatic test BIOLABO® (Maizy, France). Vesicle dispersion (10

µl) was added to the reagent and obtained solution kept in an incubator for 10 minutes at 30°C and thus, analyzed at 500 nm using a UV spectrophotometer (Beckman DU 7400, Paris, France). Aggregation efficiancy (AE%) was calculated using equation 1:

Eq. 1 $AE\% = [Ph_{dialysed}]/[Ph_{undialysed}] \times 100$

were $Ph_{dialysed}$ is phospholipid concentration after dyalisis and $Ph_{undialysed}$ is phospholipid concentration before dalysis. The quantitative determination of chitosan was performed by colorimetric test based on the formation of colored complexes between the amino groups of the chitosan and the anionic groups of the Cibacron Brilliant Red 3B-A (83). Chitosan amount was measured in supernatant and precipitate after ultracentrifugation. Coating efficiency (CE%) was calculated using equation 2: Eq. 2 $CE\% = [CH_{centrifugated}]/[CH_{uncentrifugated}] \times 100$

were $CH_{centrifugated}$ is chitosan concentration after centrifugation and $CH_{uncentrifugated}$ is chitosan concentration before centrifugation. CUR entrapment efficiency (EE%), expressed as the percentage of the amount of CUR found after purification respect that initially used, was determined by UV analysis after distruption of vesicles by methanol dilution (1/500). CUR content was quantified at 424 nm using a spectrophotometer Beckman DU 7400 (Paris, France).

5.3. Calu-3 cell line culture

The Calu-3 cell line was obtained from the American Tissue Type Collection (catalog number HTB-55) and maintained at 37°C and 5% CO_2 in a humidified atmosphere. Cells were cultured in Dulbecco's modified Eagle's medium (DMEM, Lonza, Levallois, France) supplemented with 50 U/mL penicillin, 50 U/mL streptomycin, and 10% fetal bovine serum (Lonza, Levallois, France). The medium was changed every four days and cells were passed weekly at a 1/3 split ratio using Trypsine-EDTA.

5.3.1. Cell viability assay

The in vitro cytotoxicity of the liposomes and chitosomes was evaluated using the 3-[4,5-dimethylthiazol-2-yl]-3,5 diphenyl tetrazolium bromide (MTT) test. This assay depends on the cellular reductive capacity to metabolize the MTT to a highly colored formazan product. Cells were seeded in 200 μL of growth medium (1.25 × 105 cells/mL) in 96-well plates (TPP, Zurich, Switzerland) and preincubated for 24 hours to recover. Then, 100 μL of freshly prepared samples dispersions in fetal bovine serum-containing cell culture medium were added immediately after dilution to different drug concentrations (150-0.075 μg/mL). The formulations were assayed for toxicity over 4, 24, and 72 hours of incubation. After the incubation period, 20 μL of a 5 mg/mL MTT solution in phosphate-

buffered saline was added to each well. After 2 hours, the culture medium was gently aspirated and replaced by 200 μL of dimethyl sulfoxide in order to dissolve the formazan crystals. The absorbance of the solubilized dye, correlates with the number of living cells, was measured with a microplate reader (LAB Systems Original Multiscan MS, Helsinki, Finland) at 570 nm. All experiments were repeated at least three times and in triplicates. Results are shown as percent of cell viability in comparison with non-treated control cells (100% viability).

5.3.2. Statistical analysis of data

Results are expressed as the mean ± standard deviation (SD). Analysis of variance (ANOVA) and Bartlett's test for homogeneity of variance were performed using SPSS version 17.0 for Windows (SPSS Inc., Chicago, United States). Post hoc testing ($P < 0.05$) of multiple comparisons was performed using the Scheffe test. Differences were considered significant at the 0.05 level of probability (p).

5.4. Results and discussion

5.4.1. Liposome and Chitosome Characterization

Negative liposomes were prepared using a commercial mixture of phospholipids (P50, 60 mg/mL) and curcumin (CUR, 5 mg/mL). by Lipid mixture were hydrated with PBS, left swelling for 12 hours and

then sonicating it. To further improve stability as well as to achieve a mucoadhesive formulation, the surface of P50 liposomes was coated with CH (84). Chitosan coated liposomes (so called chitosomes) were previously prepared by several authors (51, 80, 75-77)

Liposome and chitosomes formation and their structure were confirmed by TEM. Figure 1.

Figure 1. Negative stain electron micrographs of **(a)** curcumin loaded liposomes and **(b)** chitosomes.

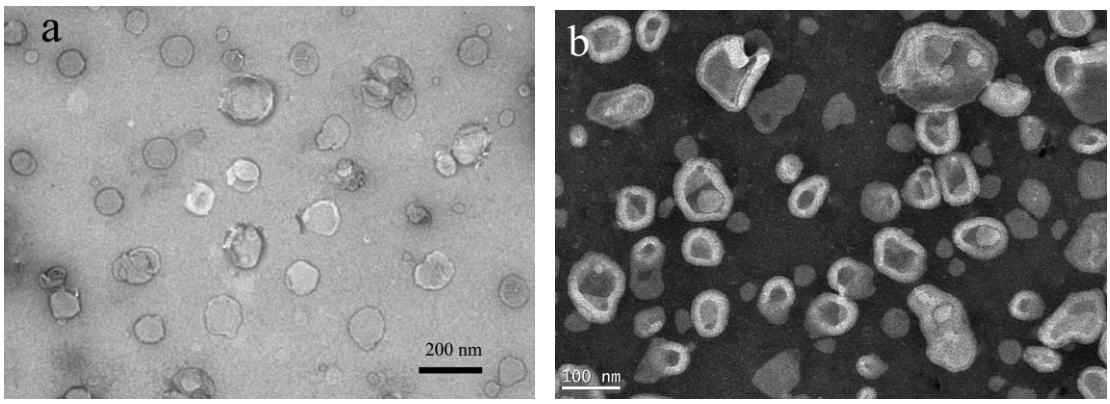

Mean size and zeta potential of liposomal formulations are shown in Table 2. Mean diameter of empty liposomes was 100±3 and samples was low polydispersed (P.I. ~ 0.18). When CUR was added in the formulation, vesicle size sligtly increased (10%) but polydispersity index became constant. Chitosome diameter increased up 199±18 nm due to the formation of coating polymer layer.

Zeta potential of liposomes was strongly negative (-51 mV, Table 2) because P50 is a mixture of phosphatidylcholine, other phospholipids

and fatty acids. At pH ~6 the negative phosphate residues of the phospholipids were distribuited to membrane surface leading a negative potential. Moreover, fatty acids, could contribute to the negative value of zeta potential (84). Positively charged polymeric CH molecules can easly interact with negative phosphate group of liposomes surface allowed stable, electrostatic interactions. The change of the zeta potential of chitosomes to positive values (+48 mV) confirmed the formation of polymer coating on the liposome surface. This strongly positive zeta potential value may represent stability against aggregation processes due to the electrostatic repulsion among vesicles in dispersion.

Table 2. Mean diameter, Polydispersity Index (PI) and Zeta Potential of empty and CUR loaded liposomes empty and CUR loaded chitosomes.

Sample		**Mean diameter (nm)**	**P.I.**	**Zeta potential (mV)**
Liposomes	empty	100±3	0.18	-58±1
Liposomes	CUR	111±3	0.17	-51±4
Chitosomes	empty	398±8	0.232	+26±1
Chitosomes	CUR	199±18	0.18	+48±2

CUR entrapped efficiency of liposomes (86%) was sligtly higher than that of chitosomes (78%) due to a lost of drug during ultracentrifugation process.

Quantitative determination of the lipids was performed using an enzymatic kit (Biolabo®) that measured only the effective amount of phosphatidylcholyne in dispersion. Using this concentration we calculated the vesicles aggregation efficiency (%). AE% of liposomes was hight (92%) confirming a good ability of phospholipipds to form closed bilayer vesicles in presence of CUR. AE% of chitosomes was lower (80%) probably because a little amount (10%) of uncoated phospholipids vesicles was lost during centrifugation procedure. In fact, too the drug EE% of chitosomes was lower than that of liposomes. The colorimetric determination of chitosan was carried before and after ultracentrifuge on the pellet and the supernatant obtained from chitosome dispersion. Chitosan coating efficiency (%) was 66%. It rapresents the effective amount of chitosan able to stably interact with vesicle surface. Chitosan on vesicle surface stabilized the dispersion and could improve vesicle mucoadhesion and drug bioavailability. However, it is important to eliminate the excess of chitosan in dispersion because it can form polymer aggregates that precipitated.

Table 3. Entrapment Efficiency (EE%), Coating Efficiency (CE%) and Aggregation Efficiency (AE%) of empty liposomes, CUR loaded liposomes and chitosomes.

Sample		EE (%)	AE (%)	CE (%)
Liposomes	CUR	86±4	92±3	
Chitosomes	CUR	78±3	80±6	66±4

5.4.2. Effect of liposomes and chitosomes concentration and surface chemistry on cell viability assay

Calu-3 cell viability was studied as a function of drug concentration (0.15-0.00075 μg/mL) using the MTT assay. This quantitative colorimetric test is based on the ability of viable cells to metabolize the water-soluble dye (MTT) into a colored formazan salt. Liposomes toxicity and cell viability was investigated for 4, 24 and 72 hours. After incubation with CUR loaded liposomes cell viability was always higher than 80% even at the highest drug concentrations. Cell viability was not compromise by drug and phospholipids concentration (Figure 2). Chitosomes toxicity was very low at 4 hours of incubation and the association between phospholipids and chitosan seem to reduce the toxicity and stimulate cell proliferation (Figure 3).

Figure 2. Calu-3 cell viability (MTT assay) after exposure to **(a)**curcumin loaded liposomes, and **(b)** chitosomes as a function of time. Each experiment was repeated for three times. Results are expressed as percentages of absorption for treated cells (±standard deviation) in comparison with untreated control cells.

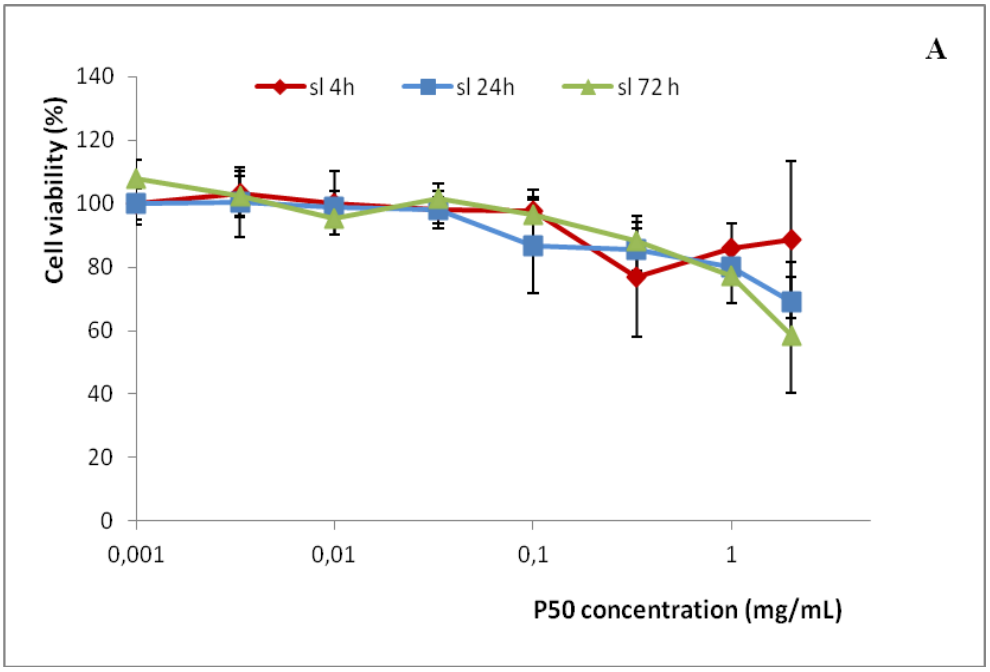

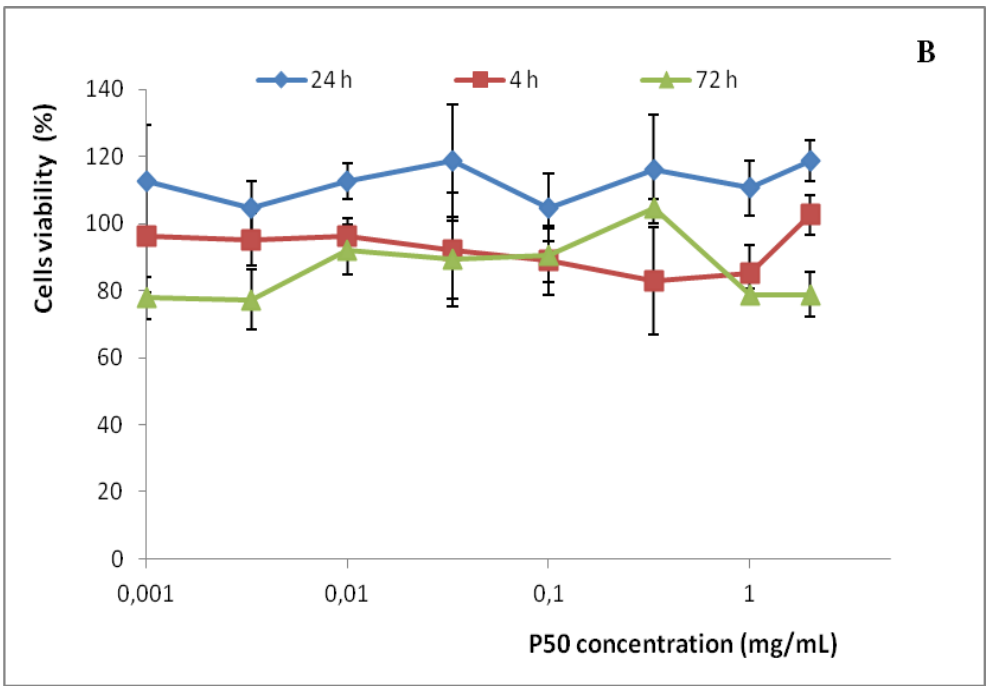

Successively, viability decreased gradually. Chronical exposure of cells (72 h) to chitosomes increased cell mortality up to 80% compared to untreated control cells (100% viability). Also in this case cell viability was not affect by drug, phospholipids and chitosan concentrations. For both the tested formulations the toxicicy was always acettable and mortality did not overcam 20% except for the highest drug and phospholipids concentrations (drug 0.15 μg/ml). The presence of chitosan in formulation did not change mortality values.

5.5. Conclusions

Chitosomes were prepared by using a mixture of fluid soy phosphatidylcholine and others fatty acids (P50), chitosan as coating polymer have a mean diameter around 200 nm that is suitable for pulmonary delivery. They showed a good capability to incorporate high quantity of curcumin also retained in high amount after the coating procedure. Chitosomes induce low toxicity even at hight concentration and time retentions in Calu-3 cells. These outcomes represent a base condition for further studies, in order to evaluate their biological properties and to assess in vivo activity in infected animal models.

6.0. Final discussion

In this thesis work were prepared and characterized liposomes and liposomes modified with a coating of chitosan called chitosomes. Through these structures were conveyed drugs of natural origin with anti-inflammatory and antioxidant properties: quercetin,phycocyanin and curcumin. The liposomes loading quercetin and phycocyanin are designed for a topical application and were tested on new born pig skin. Liposomes and chitosomes loading curcumin are designed for pulmonary delivery as a cure for cystic fibrosis. In this case, has been tested the toxicity of the system using a model of lung tissue using Calu-3 cells.

The drug delivery via liposomes and chitosomes improves the retention time of the drug and increases its stability. Studies continue with biocompatibility and in vivo tests.

References

1. El Maghraby G.M.M., Williams A.C., Barry B.W. Interactions of surfactants (edge activators) and skin penetration enhancers with liposomes. International Journal of Pharmaceutics. Vol. 276, Issues 1–2, pp. 143-161, 2004.
2. I van den Bergh B.A., A. J. Bouwstra, H. Junginger, P. W. Wertz. Elasticity of vesicles affects hairless mouse skin structure and permeability. Journal of Controlled Release. Vol. 62, Issue 3-6 pp. 367-379, 1999.
3. E. Touitou, N. Dayan, L. Bergelson, B. Godin, M. Eliaz. Ethosomes — novel vesicular carriers for enhanced delivery: characterization and skin penetration properties. Journal of Controlled Release. Vol. 65, Issue 3-3, pp. 403-418, 2000.
4. M.K. Chourasia, L. Kang, S.Y. Chan. Nanosized ethosomes bearing ketoprofen for improved transdermal delivery. Results in Pharma Science. Vol. 1, pp.60-67, 2011.
5. M. Manconi,S. Mura, C. Sinico, A.M. Fadda, A.O. Vila, F. Molina. Development and characterization of liposomes containing glycols as carriers for diclofenac. Colloids and Surfaces A: Physicochemical and Engineering Aspects. Vol. 342, pp. 53-58, 2009.
6. Manconi, M.; Sinico, C.; Caddeo, C.; Vila, A.O.; Valenti, D.; Fadda, A.M. Penetration enhancer containing vesicles as carriers

for dermal delivery of tretinoin. Int. J. Pharm. Vol. 412, pp. 37-46, 2011.

7. M. Manconi, C. Caddeo, C. Sinico, D. Valenti, M.C. Mostallino, G. Biggio, A.M. Fadda, Ex vivo skin delivery of diclofenac by transcutol containing liposomes and suggested mechanism of vesicle-skin interaction, Eur. J. Pharm. Biopharm. Vol. 78, pp. 27-35, 2011.
8. S. Mura, M. Manconi, C. Sinico, D. Valenti and A.M. Fadda, Penetration enhancer containing vesicles (PEVs) as carriers for cutaneous delivery of minoxidil. Int. J. Pharm. Vol. 380, pp. 72-79, 2009.
9. S. Mura, M. Manconi, D. Valenti, C. Sinico, A.O. Vila and A.M. Fadda, Transcutol containing vesicles for topical delivery of minoxidil, J. Drug Target. Vol. 19, pp. 189-196, 2011.
10. S. Mura, H. Hillaireau, N. Tsapis, E. Fattal. Influence of surface charge on the potential toxicity of PLGA nanoparticles towards Calu-3 cells. International Journal of nanomedicine. Vol. 6, pp. 2591-2605, 2011.
11. M. Chessa, C. Caddeo, D. Valenti, M. Manconi, C. Sinico and A.M. Fadda, Effect of Penetration Enhancer containing Vesicles on the percutaneous delivery of quercetin through new born pig skin, Pharmaceutics. Vol. 3, pp. 497-509, 2011.
12. C. Caddeo, M. Manconi, D. Valenti, A.M. Maccioni, A.M. Fadda, C. Sinico. The role of Labrasol® in the enhancement of

the cutaneous bioavailability of minoxidil in phospholipid Vesicles. Research Journal of Pharmacy and Technology. Vol.5, pp. 1563-1569, 2012.

13. P.M. Elias, D.S. Friend, The permeability barrier in mammalian epidermis, J. Cell Biol. Vol. 65 pp. 180–191, 1975.
14. P.M. Elias, G.K. Menon, Structural and lipid biochemical correlates of the epidermal permeability barrier, Adv. Lipid Res. Vol. 24, pp. 1–26, 1991.
15. A.S. Michaels, S.K. Chandrasekaran, J.E. Shaw, Drug permeation through human skin: theory and in vitro experimental measurement, AlChE J. Vol. 21, pp. 985–986, 1975.
16. K.M. Hanson, M.J. Behne, N.P. Barry, T.M. Mauro, E. Gratton, R.M. Clegg, Twophoton fluorescence lifetime imaging of the skin stratum corneum pH gradient, Biophys. J. Vol. 83, pp. 1682–1690, 2002.
17. R.O. Potts, R.H. Guy, A predictive algorithm for skin permeability: the effects of molecular size and hydrogen bond activity, Pharm. Res. Vol. 12, pp. 1628–1633, 1995.
18. D. van der Merwe, J.D. Brooks, R. Gehring, R.E. Baynes, N.A. Monteiro-Riviere, J.E. Riviere, A physiologically based pharmacokinetic model of organophosphate dermal absorption, Toxicol. Sci. Vol. 89, pp. 188–204, 2006.

19. B. Baroli, M.G. Ennas, F. Loffredo, M. Isola, R. Pinna, M.A. Lopez-Quintela, Penetration of metallic nanoparticles in human full-thickness skin, J. Invest. Dermatol. Vol. 127, pp. 1701–1712, 2007.

20. Scalia, S.; Mezzena, M. Incorporation of quercetin in lipid microparticles: Effect on photo- and chemical-stability. J. Pharm. Biomed. Anal. Vol 49, pp. 90-94, 2009.

21. L. Montenegro,C. Carbone, C. Maniscalco, D. Lambusta, G. Nicolosi,C.A. Ventura, G. Puglisi. In vitro evaluation of quercetin-3-O-acyl esters as topical prodrugs. Int. J. Pharm. Vol. 336, pp. 257-262, pp. 2007.

22. F.T. Vicentini, T.R. Simi, J.O. Del Ciampo, N.O. Wolga, D.L. Pitol, M.M. Iyomasa, M.V. Bentley, M.J. Fonseca. Quercetin in w/o microemulsion: in vitro and in vivo skin penetration and efficacy against UVB-induced skin damages evaluated in vivo. Eur. J. Pharm. Biopharm. Vol. 69, pp. 948-957, 2008.

23. M. Manconi, S. Mura, C. Sinico, A.M. Fadda, A.O. Vila, F. Molina. Development and characterization of liposomes containing glycols as carriers for diclofenac. Colloids Surf. A: Physicochem. Eng. Asp. Vol. 342,pp. 53-58, 2009.

24. M. Manconi, C. Caddeo, C. Sinico, D. Valenti, M.C. Mostallino, G. Biggio, A.M. Fadda. *Ex vivo* skin delivery of diclofenac by transcutol containing liposomes and suggested

mechanism ofvesicle–skin interaction. Eur. J. Pharm. Biopharm. Vol. 78, pp. 27-35, 2011.

25. M. Manconi, C. Sinico, C. Caddeo, A.O. Vila, D. Valenti, A.M. Fadda. Penetration enhancer containing vesicles as carriers for dermal delivery of tretinoin. Int. J. Pharm. Vol. *412*, pp. 37-46, 2011.
26. S. Mura, M. Manconi, C. Sinico, D.Valenti, A.M. Fadda. Penetration enhancer-containing vesicles (PEVs) as carriers for cutaneous delivery of minoxidil. Int. J. Pharm. Vol. 380, pp. 72-79, 2009.
27. S. Mura, M. Manconi, D. Valenti, C. Sinico, A.O. Vila, A.M. Fadda. Transcutol containing vesicles for topical delivery of minoxidil. J. Drug Targeting, Vol. 19, pp. 189-196, 2011.
28. M. Manconi, J. Aparicio, D. Seyler, A.O. Vila, J. Figueruelo, F. Molina. Effect of several electrolytes on the rheopectic behaviour of concentrated soy lecithin dispersions. Colloids Surf. APhysiochem. Eng. Asp. Vol. 270, pp. 102-106, 2005
29. C. Caddeo, K. Teskac, C. Sinico, J. Kristl, J. Effect of resveratrol incorporated in liposomes on proliferation and UV-B protection of cells. Int. J. Pharm. Vol. 363, pp. 183-191, 2008.
30. A. Gonzalez-Paredes, M. Manconi, C. Caddeo, A. Ramos-Cormenzana, M. Monteoliva-Sanchez, A.M. Fadda. Archaeosomes as carriers for topical delivery of betamethasone

dipropionate: *in vitro* skin permeation study. J. Lipos. Res. Vol. 20, pp. 269-276, 2010.

31. D. Robertson, T. Hellweg, B. Tiersch, J. Koetz. Polymer-induced structural changes in lecithin/sodium dodecyl sulfate-based multilamellar vesicles. J. Colloid Interface Sci. Vol. 270, pp. 187-194, 2004.
32. J.A. Bouwstra, P.L. Honeywell-Nguyen. Skin structure and mode of action of vesicles. Advan. Drug Delivery Rev. Vol. 54, pp. 41-55, 2002.
33. P.L. Honeywell-Nguyen, H.W.W. Groenink, J.A. Bouwstra. Elastic vesicles as a tool for dermal and transdermal delivery. J. Lipos. Res. Vol. 16, pp. 273-280, 2006.
34. M. Brunner, P. Dehghanyar, B. Seigfried, W. Martin, G. Menke and M. Müller. Favourable dermal penetration of diclofenac after administration to the skin using a novel spray gel formulation, Br. J. Clin. Pharmacol. Vol. 60, pp. 573-577, 2005.
35. I. Tegeder, U. Muth-Selbach, J. Lotsch, G. Rusing, R. Oelkers, K. Brune, S. Meller, G.R. Kelm, F. Sorgel and G. Geisslinger. Application of microdialysis for the determination of muscle and subcutaneous tissue concentrations after oral and topical ibuprofen administration. Clin. Pharmacol. Ther. Vol. 65, pp. 357-368, 1999.

36. D. Paolino, G. Lucania, D. Mardente, F. Alhaique, M. Fresta. J. Control. Release. Vol. 106, pp. 99-110, 2005.

37. G. Nava, E. Piñón, L. Mendoza, N. Mendoza, D. Quintanar and A. Ganem. Formulation and *in Vitro*, *ex Vivo* and *in Vivo* Evaluation of Elastic Liposomes for Transdermal Delivery of Ketorolac Tromethamine. Pharmaceutics Vol. 3, pp. 954-970, 2011.

38. L. Tavano, R. Muzzalupo, S. Trombino, R. Cassano, A. Pingitore, N. Picci. Effect of formulations variables on the in vitro percutaneous permeation of sodium diclofenac from new vesicular systems obtained from pluronic triblock copolymers. Colloid Surf. B-Biointerfaces. Vol. 79, pp. 227-234, 2010.

39. D. Paolino, R. Muzzalupo, A. Ricciardi, C. Celia, N. Picci, M. Fresta. In vitro and in vivo evaluation of Bola-surfactant containing niosomes for transdermal delivery. Biomed. Microdevices. Vol. 9, pp. 421-433, 2007.

40. S. Mura, F. Pirot, M. Manconi, F. Falson, A.M. Fadda, Liposomes and niosomes as potential cariers for dermal delivery of minoxidil. J. Drug Target. Vol. 15, pp. 101-108, 2007.

41. C. Celia, F. Cilurzo, E. Trapasso, D. Cosco, M.Fresta, D. Paolino, Ethosomes® and transfersomes® containing linoleic acid: Physicochemical and technological features of topical drug delivery carriers for the potential treatment of melasma disorders. Biomed. Microdevices. Vol. 14, pp. 119-130, 2012.

42. M.M.A. Elsayed, O.Y. Abdallah, V.F. Naggar and N.M. Khalafalla. PG-liposomes: Novel lipid vesicles for skin delivery of drugs. J. Pharm. Pharmacol. Vol.59, pp. 1447-1450, 2007.

43. N. Dragicevic-Curic, D. Scheglmann, V. Albrecht and A. Fahr. Development of different temoporfin-loaded invasomes-novel nanocarriers of temoporfin: characterization, stability and in vitro skin penetration studies. Colloid Surf. B-Biointerfaces Vol. 70, pp. 198-206, 2009.

44. M. Manconi, S. Mura, C. Sinico, A.M. Fadda, A. Vila, F. Molina. Development and characterization of liposomes containing glycols as carriers for diclofenac. Colloid Surf. A-Physicochem. Eng.Vol. 342, pp. 53-58, **2009**.

45. M. Manconi, C. Caddeo, C. Sinico, D. Valenti, M.C. Mostallino, G. Biggio, A.M. Fadda. *Ex vivo* skin delivery of diclofenac by transcutol containing liposomes and suggested mechanism of vesicle-skin interaction, Eur. J. Pharm. Biopharm. Vol. 78, pp. 27-35, 2011.

46. M. Manconi, C. Sinico, C. Caddeo, A.O. Vila, D. Valenti, A.M. Fadda, Penetration enhancer containing vesicles as carriers for dermal delivery of tretinoin, Int. J. Pharm. Vol. 412, pp. 37-46, 2011.

47. S. Mura, M. Manconi, C. Sinico, D. Valenti and A.M. Fadda, Penetration enhancer containing vesicles (PEVs) as

carriers for cutaneous delivery of minoxidil. Int. J. Pharm. Vol. 380, pp. 72-79, 2009.

48. S. Mura, M. Manconi, D. Valenti, C. Sinico, A.O. Vila, A.M. Fadda, Transcutol containing vesicles for topical delivery of minoxidil, J. Drug Target. Vol. 19, pp. 189-196, 2011.

49. M. Manconi, C. Caddeo, C. Sinico, D. Valenti, M.C. Mostallino, S. Lampis, M. Monduzzi, A.M. Fadda, Penetration enhancer-containing vesicles: composition dependence of structural features and skin penetration ability, Eur. J. Pharm. Biopharm. Vol. 82, pp. 352-359, 2012.

50. R.M. Elmoslemany, O.Y. Abdallah, L.K. El-Khordagui, N.M. Khalafallah, Propylene Glycol Liposomes as a Topical Delivery System for Miconazole Nitrate: Comparison with Conventional Liposomes, AAPS Pharm. Sci. Tech. Vol. 13, pp. 723-731, **2012**.

51. M. Manconi, S. Mura, M. Manca, A.M. Fadda, M. Dolz, M. Hernandez, A. Casanovas, O. Diez- Chitosomes as drug delivery systems for C-phycocyanin: Preparation and characterization. Sales, Int. J. Pharm. Vol. 392, pp. 92-100 2010.

52. N.T. Eriksen, Production of phycocyanin a pigment with applications in biology, biotechnology, foods and medicine, Appl. Microbiol. Biotechnol. Vol. 80, pp. 1-14, 2008.

53. C. Romay, J. Armesto, D. Remirez, R. Gonzalez, N. Ledon and I. Garcia, Antioxidant and anti-inflammatory properties of c-

phycocyanin from blue-green algae, Inflamm. Res. Vol. 47, pp. 36-41, 1998.

54. C. Reddy, V.B. Bhat, G. Kiranmai, M. Reddy, P. Reddanna and K. Madyastha, Selective inhibition of cyclooxygenase-2 by c-phycocyanin, a biliprotein from spirulina platensis, Biochem. Bioph. Res. Co. Vol. 277, pp. 599-603, 2000.

55. M. Manconi, J. Pendás, N. Ledón, T. Moreira, C. Sinico, L. Saso and A.M. Fadda, Phycocyanin liposomes for topical anti–inflammatory activity: in-vitro in-vivo studies, J. Pharm. Pharmacol. Vol. 61, pp. 423-430, 2009.

56. H.P. Singh, P. Utreja, A.K. Tiwary and S. Jain, Elastic Liposomal Formulation for Sustained Delivery of Colchicine: *In Vitro* Characterization and *In Vivo* Evaluation of Anti-gout Activity, AAPS J. Vol. 11, pp. 54-64, 2009.

57. S. Benedetti, S. Rinalducci, F. Benvenuti, S. Francogli, S. Pagliarani, L. Giorgi, M. Micheloni, G.M. D'Amici, L. Zolla and F. Canestrari, Purification and characterization of phycocyanin from the blue-green algae *Aphanizomenon flos-aquae*, J. Chromatogr. B Vol. 883, pp. 12-18, 2006.

58. A. Shevchenko, M. Wilm, O. Vorm and M. Mann, Mass spectrometric sequencing of proteins from silver stained polyacrylamide gels, Anal. Chem. Vol. 68, pp. 850-858, 1996.

59. C. Caddeo, K. Teskač, C. Sinico and J. Kristl, Effect of resveratrol incorporated in liposomes on proliferation and UV-B protection of cells, Int. J. Pharm. Vol. 363, pp. 183-191, 2008.

60. M. Chessa, C. Caddeo, D. Valenti, M. Manconi, C. Sinico and A.M. Fadda, Effect of Penetration Enhancer containing Vesicles on the percutaneous delivery of quercetin through new born pig skin, Pharmaceutics Vol. 3, pp. 497-509, 2011.

61. G. Pabst, M. Rappolt, H. Amenitsch and P. Laggner, Structural information from multilamellar liposomes at full hydration: full q-range fitting with high quality X-ray data, Phys. Rev. E Stat. Phys. Plasmas Fluids Relat. Interdiscip. Top. Vol. 62, pp. 4000-4009, 2000.

62. H. Madhyastha, K. Radha, M. Sugiki, S. Omura and M. Maruyama, Purification of c-phycocyanin from spirulina fusiformis and its effect on the induction of urokinasetype plasminogen activator from calf pulmonary endothelial cells, Phytomedicine. Vol. 13, pp. 564-569, 2006.

63. S. Rinalducci, P. Roepstorff and L. Zolla, De novo sequence analysis and intact mass measurements for characterization of phycocyanin subunit isoforms from the blue-green alga Aphanizomenon flos-aquae, J. Mass. Spectrom. Vol. 44, pp. 503-515, 2009.

64. T. Chen, Y.-S. Wong and W. Zheng, Purification and characterization of selenium-containing phycocyanin from

selenium-enriched Spirulina platensis, Phytochemistry Vol. 67, pp. 2424-2430, 2006.

65. S.-G. Yan, L.-P. Zhu, H.-N. Su, X.-Y. Zhang, X.-L. Chen, B.-C. Zhou and Y.-Z. Zhang, Single-step chromatography for simultaneous purification of C-phycocyanin and allophycocyanin with high Weibel E. Morphometrics of the lung. Handbook of physiology, Washington DC: American Physiological Society. Vol 1, pp. 285, 1964

66. Purity and recovery from Spirulina (Arthrospira) platensis, J. Appl. Phycol. Vol. 23, pp. 1-6, 2011.

67. M. Manconi, R. Isola, A.M. Falchi, C. Sinico and A.M. Fadda, Intracellular distribution of fluorescent probes delivered by vesicles of different lipidic composition, Colloid Surf. B-Biointerfaces Vol. 57, pp. 143-151, 2007.

68. X. Xu, M.A. Khan and D.J. Burgess, Predicting hydrophilic drug encapsulation in unilamellar liposomes, Int. J. Pharm. Vol. 423, pp. 410-418, 2012.

69. E. Touitou, N. Dayan, L. Bergelson, B. Godin and M. Eliaz, Ethosomes novel vesicular carriers for enhanced delivery: characterization and skin penetration properties, J. Control. Release Vol. 65, pp. 403-418, 2000.

70. D. Ainbinder, D. Paolino, M. Fresta and E. Touitou, Drug Delivery Applications with Ethosomes, J. Biomed. Nanotechnol. Vol. 6, pp. 558-568, 2010.

71. G. Tan, P. Xu, L.B. Lawson, J. He, L.C. Freytag, J.D. Clements and V.T. John, Hydration effects on skin microstructure as probed by high-resolution cryo-scanning electron microscopy and mechanistic implications to enhanced transcutaneous delivery of biomacromolecules, J. Pharm. Sci. Vol. 99, pp. 730-740, 2010.

72. M. Zaru, S. Mourtas, P. Klepetsanis, A.M. Fadda, S.G. Antimisiari. Liposomes for drug delivery to the lungs by nebulization. Eur J Pharm Biopharm Vol. 67, pp. 655-666, 2007.

73. S.P. Vyas, M.E. Kannan, S. Jain, V. Mishra, P. Singh P. Design of liposomal aerosols for improved delivery of rifampicin to alveolar macrophages. Int J Pharm Vol. 269, pp. 37–49, 2004.

74. M. Zaru, C. Sinico, A. De Logu, C. Caddeo, F. Lai, M.L. Manca, A.M. Fadda. Rifampicin-loaded liposomes for the passive targeting to alveolar macrophages: in vitro and in vivo evaluation. J Lip Res Vopl. 19, pp. 68-76, 2009.

75. S. Madrigal-Carballo, A.O. Vila, M. Sibaja, J.D. Reed, F. Molina. In vitro uptake of lysozyme-loaded liposomes coated with chitosan biopolymer as model immunoadjuvants. J Liposome Res. Vol. 20, pp. 1-8, 2010.

76. M.L. Manca, M. Manconi M, D. Valenti, F. Lai, G. Loy, P. Matricardi, A.M. Fadda. Liposomes coated with chitosan–xanthan gum (chitosomes) as potential carriers for pulmonary

delivery of rifampicin. J Pharm Sci. Vol. 101, pp. 566-575, 2012.

77. M. Zaru, M.L. Manca, A.M. Fadda, S.G. Antimisiaris. Chitosan-coated liposomes for delivery to lungs by nebulization. Colloid Surface B Vol. 71, pp. 88-95, 2009.

78. J. Lipecka, C. Norez, N. Davezac., et al. Rescue of ΔF508-CFTR (Cystic Fibrosis Transmembrane Conductance Regulator) by Curcumin: Involvement of the Keratin 18 Network. The Journal of pharmacology and experimental therapeutics. Vol. 317, pp. 500-505, 2006.

79. A.L. Berger, C.O. Randak, P.H. Karp P.H., et al. Curcumin stimulates fibrosis transmembrane conductance regulator CL-channel activity. The journal of biological chemistry. Vol. 280, pp. 5221-5226, 2005.

80. S. Channarong, W. Chaicumpa, N. Sinchaipanid, A. Mitrevej. Development and Evaluation of Chitosan-Coated Liposomes for Oral DNA Vaccine: The Improvement of Peyer's Patch Targeting Using a Polyplex-Loaded Liposomes. AAPS PharmSciTech. Vol. 12, pp. 192-200, 2011.

81. M.M. Mady, M.M. Darwish. Effect of chitosan coating on the characteristics of DPPC liposomes. J Adv Res. Vol. 1, pp. 187-191, 2010.

82. S. Mura, H. Hillaireau, N.Tsapis, E. Fattal, Influence of surface charge on the potential toxicity of PLGA nanoparticles

towards Calu-3 cells. International Journal of nanomedicine. Vol. 6, pp. 2591-2605, 2011.

83. R.A. Muzzarelli. Colorimetric determination of chitosan. Analitical Biochemistry. Vol 260, pp. 255-257.

84. J. Zhuang, Q. Ping, Y. Song, Qi J, Z. Cui. Effects of chitosan coating on physical properties and pharmacokinetic behavior of mitoxantrone liposomes. Int J Nanomed. Vol. 5, pp. 407-416, 2010.